www.coinweb.no

SINTEF Building and Infrastructure Klaartje De Weerdt, Tone Østnor and Harald Justnes

Microstructure of clinker – fly ash interactions

COIN project report 69 – 2015

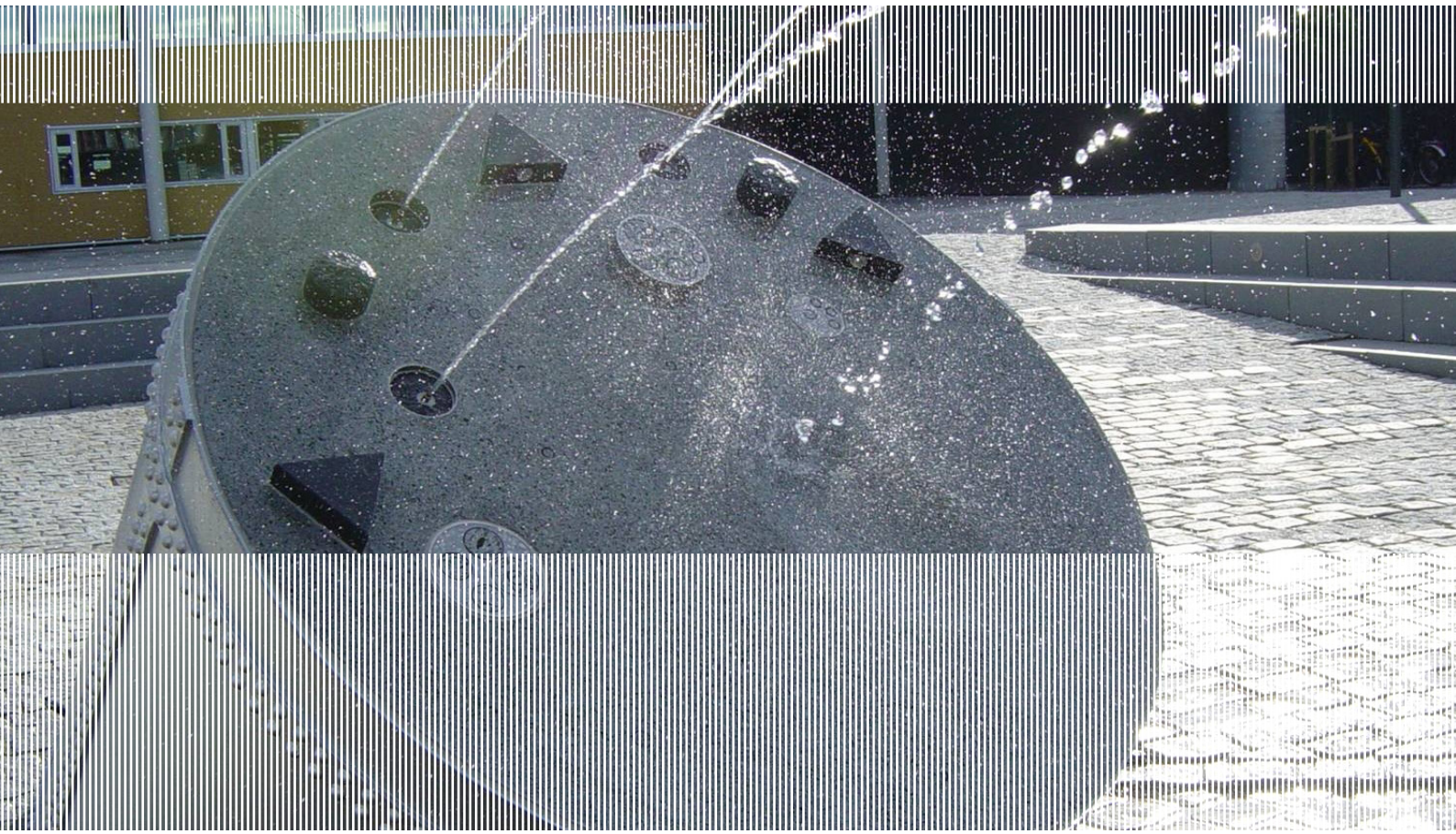

SINTEF

SINTEF Building and Infrastructure

Klaartje De Weerdt, Tone Østnor and Harald Justnes

Microstructure of clinker – fly ash interactions

FA 1 Environmentally friendly concrete

SP 1.1 Low carbon-footprint binder systems

COIN Project report 71 – 2015

COIN Project report no 69
Klaartje De Weerdt, Tone Østnor and Harald Justnes
Microstructure of clinker – fly ash interactions
FA 1 Environmentally friendly concrete
SP 1.1 Low carbon-footprint binder systems

Keywords:
Cement, fly ash, clinker

Project no.: 102000442-1

Photo, cover:
«Sculptur, Utsmykning Byåsen vgs», artist: Kari Elise Mobeck (photographer)

ISSN 1891–1978 (online)
ISBN 978-82-536-1469-4 (pdf)

Address: Forskningsveien 3 B
POBox 124 Blindern
N-0314 OSLO
Tel: +47 73 59 30 00
Fax: +47 22 69 94 38

www.sintef.no/byggforsk
www.coinweb.no

Cooperation partners / Consortium Concrete Innovation Centre (COIN)

Kværner Engineering
Contact: Jan-Diederik Advocaat
Email: Jan-Diederik.Advocaat@kvaerner.com
Tel: +47 67595050

Saint Gobain Weber
Contact: Geir Norden
Email: geir.norden@saint-gobain.com
Tel: +47 22887700

Norcem AS
Contact: Terje Rønning
Email: terje.ronning@norcem.no
Tel: +47 35572000

NTNU
Contact: Terje Kanstad
Email: terje.kanstad@ntnu.no
Tel: +47 73594700

Mapei AS
Contact: Trond Hagerud
Email: trond.hagerud@mapei.no
Tel: +47 69972000

SINTEF Building and Infrastructure
Contact: Tor Arne Hammer
Email: tor.hammer@sintef.no
Tel: +47 73596856

Skanska Norge AS
Contact: Sverre Smeplass
Email: sverre.smeplass@skanska.no
Tel: +47 40013660

Norwegian Public Roads Administration
Contact: Kjersti K. Dunham
Email: kjersti.kvalheim.dunham@vegvesen.no
Tel: +47 22073940

Unicon AS
Contact: Stein Tosterud
Email: stto@unicon.no
Tel: +47 22309035

Veidekke Entreprenør ASA
Contact: Christine Hauck
Email: christine.hauck@veidekke.no
Tel: +47 21055000

Preface

This study has been carried out within COIN - Concrete Innovation Centre - one of presently 14 Centres for Research based Innovation (CRI), which is an initiative by the Research Council of Norway. The main objective for the CRIs is to enhance the capability of the business sector to innovate by focusing on long-term research based on forging close alliances between research-intensive enterprises and prominent research groups.

The vision of COIN is creation of more attractive concrete buildings and constructions. Attractiveness implies aesthetics, functionality, sustainability, energy efficiency, indoor climate, industrialized construction, improved work environment, and cost efficiency during the whole service life. The primary goal is to fulfil this vision by bringing the development a major leap forward by more fundamental understanding of the mechanisms in order to develop advanced materials, efficient construction techniques and new design concepts combined with more environmentally friendly material production.

The corporate partners are leading multinational companies in the cement and building industry and the aim of COIN is to increase their value creation and strengthen their research activities in Norway. Our over-all ambition is to establish COIN as the display window for concrete innovation in Europe.

About 25 researchers from SINTEF (host), the Norwegian University of Science and Technology - NTNU (research partner) and industry partners, 15 - 20 PhD-students, 5 - 10 MSc-students every year and a number of international guest researchers, work on presently eight projects in three focus areas:

- Environmentally friendly concrete
- Economically competitive construction
- Aesthetic and technical performance

COIN has presently a budget of NOK 200 mill over 8 years (from 2007), and is financed by the Research Council of Norway (approx. 40 %), industrial partners (approx 45 %) and by SINTEF Building and Infrastructure and NTNU (in all approx 15 %).

For more information, see www.coinweb.no

Tor Arne Hammer
Centre Manager

Summary

The first objective was to find out why a white clinker from previous studies has a higher strength potential than the other 3 clinkers tested in the same study, as well as finding out whether or not it contains other aluminate compounds than C_3A.

Clinker δ gives higher early strength than the other clinkers because it contains anhydrite as flux and therefore has a total higher calcium sulphate content than the other cements when the same amount of gypsum is added to the clinkers.

Clinker δ also has a higher C_3A content (≈ 6%) than predicted from the Rietveld analysis and part of it probably as a glassy XRD amorphous phase with some fluorine.

Clinker δ only has a marginally higher surface than the other clinkers, but substantially higher C_3S content that will add to the higher early strength together with excess calcium sulphate not bound early by C_3A being able to help accelerate C_3S hydration.

The other clinkers also contained substantially amounts of C_4AF that has a slow hydration with large amounts remaining unhydrated at 28 days.

The second objective was to find out why one particular ash out of 4 tested gave much higher strength than the others when replacing cement (clinker with gypsum) in mortars.

Fly ash D is not a real fly ash, but a fluidized bed ash that consist of a much more open structure than the closed glassy, spherical particles of the other fly ashes. It also contains a lot more calcium oxide (17.9% CaO) than the other fly ashes (Fly ash B is the second highest with 7.1% CaO). Hence it is assumed to be more reactive than the other ashes.

Fly ash D also contains considerable more sulphate (6.6% as SO_3) than the other fly ashes (fly ash B is the second highest with 0.5% SO_3) which would lead to more ettringite formed on the expense of AFm resulting in more water bound and hence higher strength.

The higher sulphate content (and partly less aluminate) for fly ash D compared to the other fly ashes also leads to a less response of this fly ash to the synergy effect with limestone, since AFt is stabilized on the expense of AFm.

Table of contents

1 Introduction

1.1 Objectives

The first objective is to find out why a white clinker from previous studies has a higher strength potential than the other 3 clinkers tested in the same study, as well as finding out whether or not it contains other aluminate compounds than C_3A.

The second objective is to find out why one particular ash out of 4 tested gave much higher strength than the others when replacing cement (clinker with gypsum) in mortars.

1.2 Background

In a former study [1] on ternary cements based on clinker, fly ash and limestone, it was found that particular clinker δ achieved a much higher strength than the other clinkers (see Figures 1 and 2), and that there also was a quite large discrepancy between the C_3A content estimated by Bogue calculations (Table 3) from the chemical compositions in Table 1 and that observed by Rietveld analyses of XRD (Table 2) compared with the other clinkers (α, β and γ). Therefor the microstructure of clinker δ was investigated closer in order to find reasons for the higher strength development as well as to identify any other aluminate containing compounds than those assumed by Bogue calculations. For instance was the formation of a glassy (no-crystalline) calcium aluminate not observable by XRD put forward as a hypothesis.

It was also found [1] that in particular one of the four ashes (ash D) combined with the clinkers gave higher strength than the others (see Figure 3), so the second objective was to find the reason for this through investigation of the microstructure of the mortars tested for strength. Ash D also deviated strongly from ashes A, B, and C in its total chemical composition as shown in Table 4 as well as in their glass compositions in Table 5.

Table 1 Chemical composition (%) and physical properties of the clinkers

Cements	**α**	**β**	**γ**	**δ**
SiO_2	20.3	21.3	21.8	23.4
Al_2O_3	5.7	5.4	4.3	4.0
Fe_2O_3	3.3	3.9	5.6	0.2
CaO	61.3	63.5	61.4	67.0
MgO	2.9	1.9	2.1	1.1
K_2O	1.2	0.4	0.4	0.5
Na_2O	0.5	0.3	0.3	0.0
SO_3	1.5	0.4	1.2	1.6
LOI 950°C	1.9	0.5	0.5	0.7
Sum above	98.6	97.6	97.6	98.5
Blaine (m^2/kg)	449	432	426	457
Density (g/cm^3)	3.1	3.1	3.2	3.1

Table 2 XRD-Rietveld analysis of the clinker phases (%)

cements	**α**	**β**	**γ**	**δ**
C_3S	49.1	59.9	45.6	63.6
C_2S	25.6	18.8	33.3	30.3
C_3A	10.0	4.6	0.3	3.2
C_4AF	10.2	14.1	18.5	0.0
Sum	94.9	97.4	97.7	97.1

Table 3 Mineral composition of the clinkers from Bogue-calculations based on the oxide compositions in Table 1.

cements	**α**	**β**	**γ**	**δ**
C_3S	52.3	54.8	47.4	67.8
C_2S	18.8	19.8	26.8	16.0
C_3A	9.5	7.7	1.9	10.3
C_4AF	10.0	11.8	17.0	0.6
Sum	94.9	97.4	97.7	97.1

Table 4 Chemical composition (%) and physical properties of the fly ashes

Fly ash	**A**	**B**	**C**	**D**
SiO_2	52.9	47.6	53.7	38.7
Al_2O_3	26.4	27.8	22.7	19.6
Fe_2O_3	6.3	5.5	5.7	6.0
CaO	3.3	7.2	5.1	17.9
MgO	2.8	2.3	2.3	2.0
K_2O	3.0	1.4	2.1	2.5
Na_2O	1.0	0.6	1.0	0.7
SO_3	0.2	0.5	0.2	6.6
LOI	1.8	3.3	4.5	3.4
Sum above	97.7	96.2	97.3	97.4
Blaine (m^2/kg)	250	400	395	734
Density (g/cm^3)	2.2	2.4	2.3	2.6

Table 5 Glass composition (%) of the fly ashes

Fly ash	**A**	**B**	**C**	**D**
SiO_2	38.0	30.1	39.4	26.3
Al_2O_3	15.6	10.3	13.9	19.6
Fe_2O_3	4.3	5.5	6.6	6.6
CaO	2.4	5.6	4.7	11.5
MgO	2.8	2.3	2.3	2.3
K_2O	3.0	1.4	3.0	3.0
Na_2O	1.0	0.6	0.5	0.5
Sum above	67.1	55.9	70.4	69.8
total amorphous	*69.6*	*59.1*	*73.2*	*64.5*

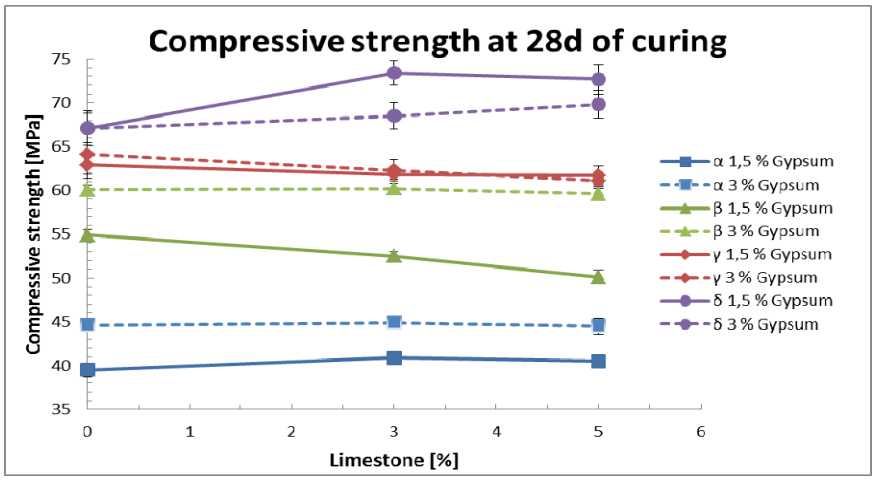

Fig. 1 Comparative plots of compressive strength at 28 days for all clinkers with 2 levels of gypsum as a function of limestone powder content.

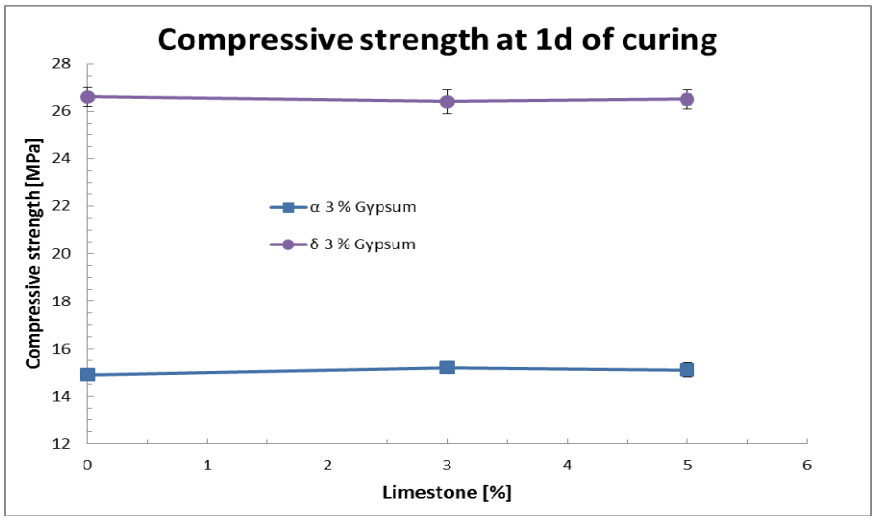

Fig. 2 Comparative plots of compressive strength at 1 day for clinkers α and δ with 3% gypsum as a function of limestone powder content.

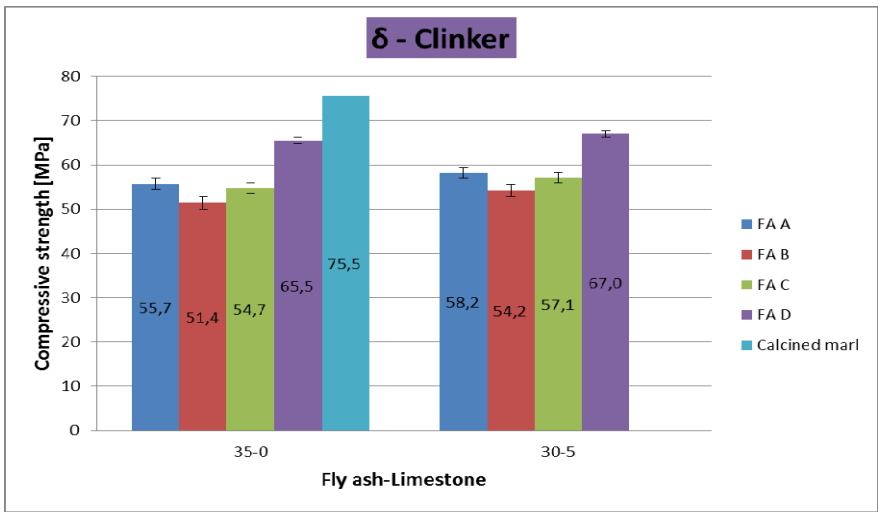

Fig. 3 The effect of different fly ashes on the compressive strength of clinker δ and their response to combination with lime stone powder. The result is also compared to 35% calcined "marl" replacing the clinker with 3% gypsum.

2 Experimental

2.1 Extraction of interstitials of clinkers

The extraction procedure involves adding 5 g dry cement to a solution of 25 g maleic acid dissolved in 125 g methanol. After stirring for 10 minutes, the solution is filtered off and the residue washed with 50 ml methanol. The procedure removes C_3S and C_2S from the clinker.

2.2 Scanning electron microscopy

One sample from all the mortar mixes cured for 28 days were cast in epoxy resin, plane polished to achieve a cross-section of the material and sputtered with carbon. The clinkers were just stirred out in epoxy resin, cut after hardening and plane polished.

The instrument used for clinkers and initial mortar studies (Figs. 15 and 16) was JEOL JXA – 8500F Electron Probe Micro analyser. The samples were analysed in the BSE (back scattered electron) mode where dense compounds and/or compounds composed of heavy elements appear bright (e.g. unreacted C_4AF mineral in cement) and compounds of low density and/or composed of elements with low atomic number appears dark (e.g. CSH). Details of interest were first checked for elements by EDS (energy dispersive spectra) semi-quantitatively, and further quantitatively by WDS (wave length dispersive spectra) for compositional determination.

A JEOL JSM-7001F field emission scanning electron microscope combined with a Genesis energy dispersive spectrometer (EDS) operated at an accelerating voltage of 15 kV was used for the SEM-EDS analysis. In each sample 120-150 EDS point analyses were performed.

2.3 X-ray diffraction (XRD)

X-ray diffraction (XRD) scan using a Bruker AXS D8 Focus with a Lynxeye super speed detector operating at 40 kV and 40 mA. A CuK_α source ($\lambda = 1.5418$ Å) with a 0.2 mm slit was used. The scan was performed between 5 and 75° 2θ with an increment of 0.02 and a scanning speed of 0.5 s/step. The samples were front loaded.

2.4 X-ray fluorescence (XRF)

After heating for mass loss on ignition (LOI), the powder is made into a tablet by melting with borax and the amount of elements detected by BRUKER S8 Tiger 4 kW X-ray spectrometer.

3 Results and discussion

3.1 Investigation of clinker

3.1.1 SEM of clinker

The back scattered electron (BSE) images of clinker δ is shown in Figure 4, while similar image for the other clinkers are reproduced in Figure 5 for comparison. In Figure 4, the black areas are epoxy in which cement grains are embedded before cutting and polishing. The lighter grey areas of the grains are the calcium silicates (alite or belite) while the slightly darker grey areas are the interstitials (in case of δ clinker only calcium aluminate, no ferrite). Note that within the calcium aluminate region there are two distinct phases in some cases (e.g. the marks D8 and D9).

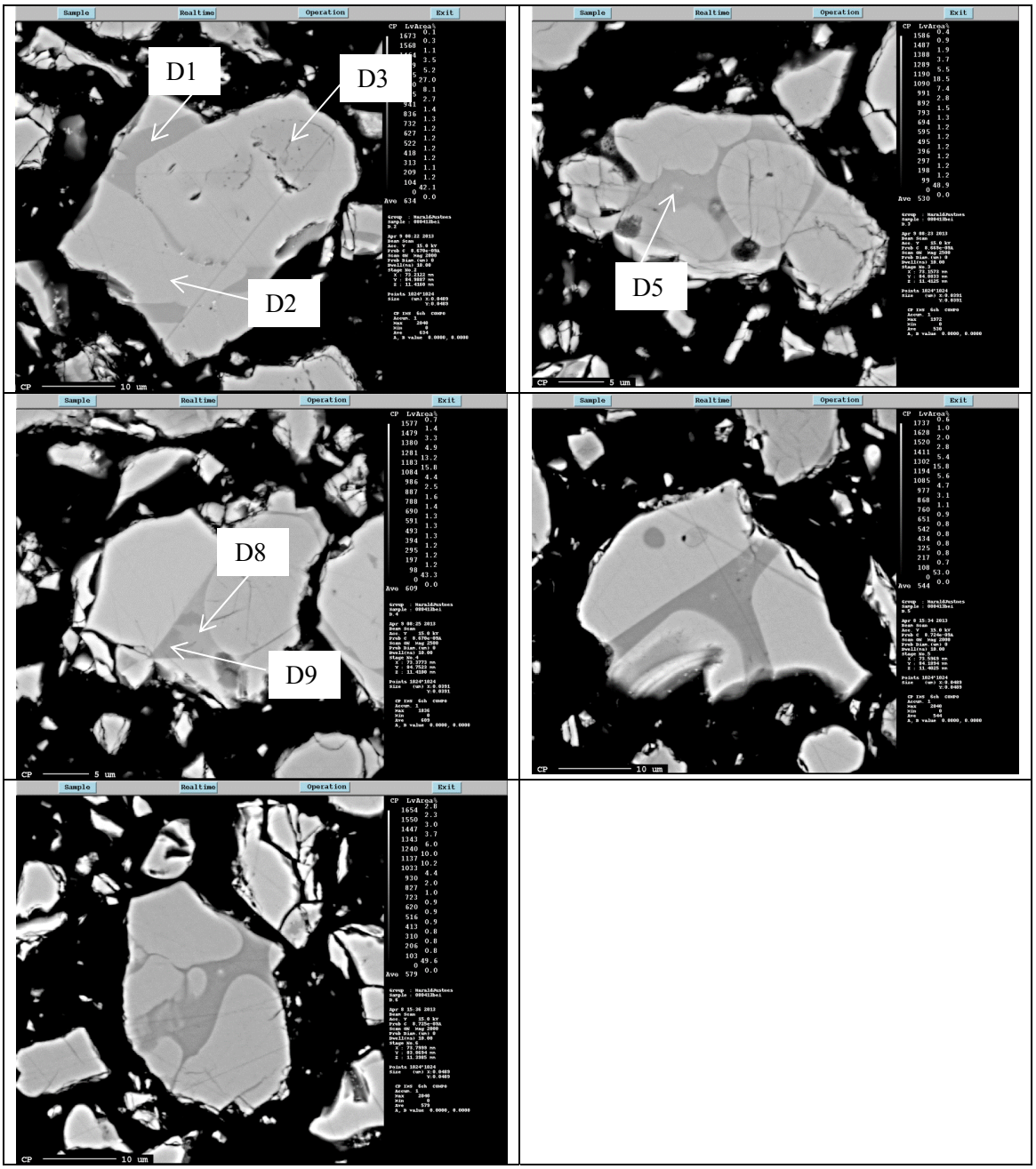

Fig. 4 BSE by SEM of various grains of the δ-clinker. The arrows signify points where 1 μm^3 was analyzed by WDS (wave length dispersive spectroscopy) and symbols refer to Table 6.

Table 6 Selected points for WDS analyses in Clinker δ. Some points are shown in Fig. 4

Point	Na	O	K	Mg	F	Ca	Si	Al	S	Ca/Al	Ca/Si	Phase
D.1	0.07	50.99	0.01	0.45	0.00	29.74	1.64	17.09	0.01	1.74	18.13	C_3A
D.2	0.00	55.69	0.01	0.73	0.57	32.76	9.34	0.81	0.09	40.49	3.51	C_3S
D.3	0.05	56.49	0.10	0.32	0.24	29.35	11.50	1.32	0.62	22.23	2.55	C_2S
D.4	0.09	56.93	0.11	0.30	0.13	29.35	11.51	1.11	0.47	26.41	2.55	C_2S
D.5	0.04	55.38	0.11	2.20	0.63	19.00	3.55	17.42	1.66	1.09	5.35	C_2A
D.6	0.05	53.67	0.04	2.49	0.56	24.14	2.21	16.42	0.43	1.47	10.95	C_3A
D.7	0.02	57.84	0.05	0.25	0.00	29.30	11.76	0.69	0.09	42.29	2.49	C_2S
D.8	0.03	54.48	0.02	1.33	0.04	26.64	1.68	15.62	0.15	1.71	15.89	C_3A, hC
D.9	0.02	54.43	0.04	2.96	0.88	21.89	2.01	17.31	0.46	1.26	10.89	C_3A, lC
D.10	0.06	54.15	0.05	2.37	0.67	24.30	2.47	15.57	0.36	1.56	9.83	C_3A
D.11	0.06	54.68	0.06	2.34	0.52	23.40	2.20	16.34	0.40	1.43	10.66	C_3A
D.12	0.07	55.22	0.04	3.02	0.81	22.73	2.56	15.02	0.54	1.51	8.89	C_3A
D.13	0.02	56.17	0.02	0.60	0.44	32.53	9.49	0.65	0.09	50.18	3.43	C_3S
D.14	0.06	54.92	0.05	2.78	0.82	23.07	2.40	15.63	0.27	1.48	9.61	C_3A
D.15	0.04	57.48	0.08	0.32	0.00	29.16	11.56	1.04	0.32	28.17	2.52	C_2S

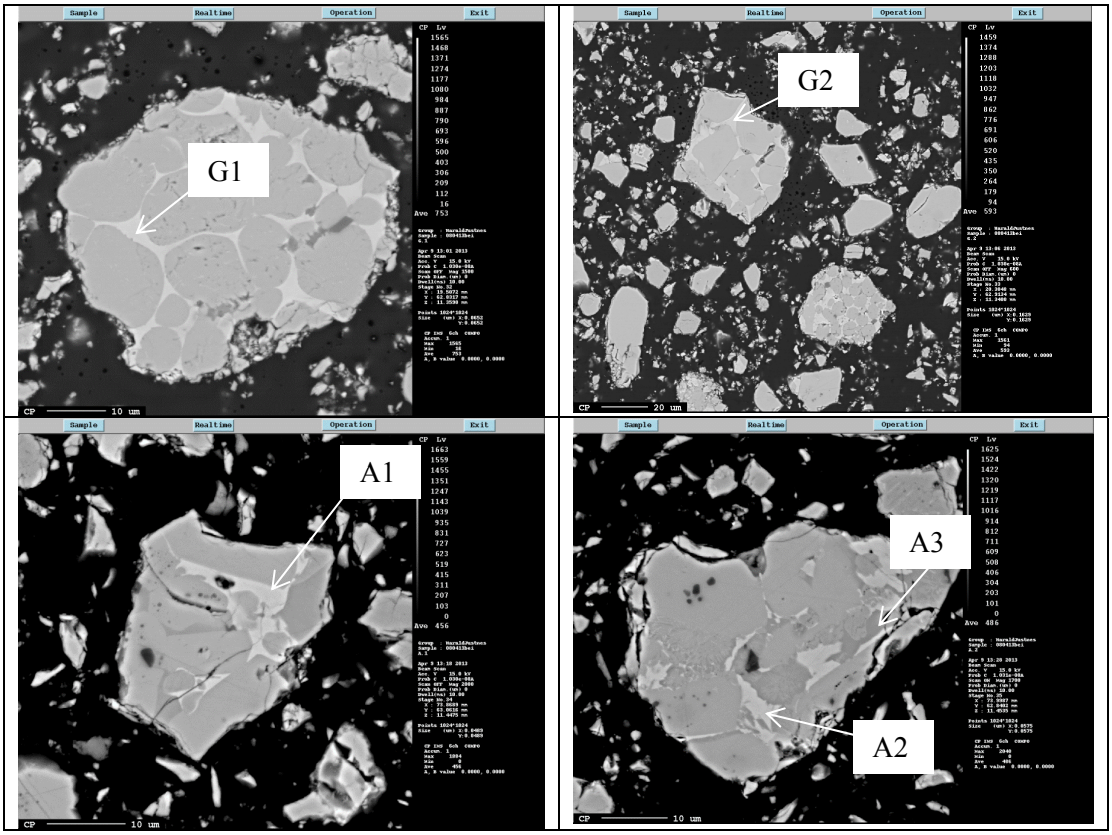

Fig. 5 BSE by SEM of various grains of the γ- and α-clinkers. The arrows signify points where 1 μm^3 was analyzed by WDS (wave length dispersive spectroscopy) and symbols refer to Table 7.

Table 7 Selected points for WDS analyses in Clinker α, β and γ. Some points are shown in Fig. 5

Point	Na	O	Fe	K	Mg	F	Ca	Si	Al	S	Ca/Al	Ca/Si	Ca/Fe	Phase
A.1	0.05	55.54	8.01	0.02	1.86	0.00	23.79	1.46	9.25	0.01	2.57	16.24	2.97	C_4AF
A.2	0.05	55.33	7.41	0.03	1.95	0.00	23.97	1.67	9.58	0.02	2.50	14.38	3.23	C_4AF
A.3	0.76	54.51	1.53	0.15	0.47	0.00	26.44	1.47	14.66	0.01	1.80	18.05	17.25	C_3A
B.1	1.46	53.59	1.77	0.11	0.28	0.00	26.64	1.23	14.91	0.01	1.79	21.62	15.07	C_3A
B.2	0.11	56.26	0.35	0.02	0.77	0.22	32.25	9.25	0.69	0.08	46.79	3.49	93.42	C_3S
B.3	0.00	53.49	8.24	0.01	1.26	0.02	24.08	0.80	12.11	0.00	1.99	29.98	2.92	C_4AF
G.1	0.00	54.17	10.50	0.01	1.69	0.17	24.25	1.40	7.78	0.02	3.12	17.26	2.31	C_4AF
G.2	0.06	54.79	9.33	0.01	1.78	0.00	24.26	1.29	8.44	0.04	2.88	18.82	2.60	C_4AF

The BSE in the upper left corner of Figure 4 shows 3 phases within one clinker δ grain being C_3S (D2), C_2S (D3) and C_3A (D1) as an example, albeit the calcium content seems to be a little high for all 3 phases (matter of calibration/reference?). The objective of the SEM analysis was actually to find out whether or not there was another calcium compound than C_3A in this clinker or if there could be a glassy, amorphous phase. Sulphur (S) and fluorine (F) was included in the analyses since it is common to use calcium fluoride, CaF_2, and even calcium sulphate, $CaSO_4$, as fluxes when iron is lacking as for this white clinker δ. The point D5 in the interstitial of the clinker grain in the upper right BSE of Figure 4 showes that this is a calcium aluminate phase with very low Ca/Al ratio (≈1 rather than 1.5) and with some silicon (3.6%), sulphur (1.7%) and fluorine (0.6%) present indicating that the above mentioned fluxes have been used. In the BSE in the middle left of Figure 4 it is obvious that the interstitial consist of two phases, one darker than the other. The analysis points are marked D8 (lighter) and D9 (darker) and the results in Table 6 reveal that the darker has higher content of Mg (3.0 vs. 1.3%), F (0.88 vs. 0.04%) and S (0.46 vs. 0.15%) and a lower atomic Ca/Al ratio (1.26 vs. 1.71) than the lighter phase.

The BSE images in the upper part of Figure 5 are of the γ clinker with analyses point G1 and G2 of the interstitial phase as indicated by the compositions in Table 7. This clinker contains no C_3A, so the interstitial should be relatively pure C_4AF which ideally should have Ca/Al = 2 and Ca/Fe = 2 if A/F = 1 as a pure phase. However the composition of C_4AF is known to vary and can also incorporate elements not analysed here (e.g. manganese, Mn).

The interstitials of the α clinker consist of a mixture of C_3A and C_4AF and BSE images of grains from this clinker is shown in the lower part of Figure 5 with analyses points A1 and A2 in the whie areas being dominated by C_4AF and a darker grey area with analysis point A3 turning out to be C_3A according to the element analyses in Table 7.

Since there are some compositional variations between similar phases, it was decided to extract the interstitials from the clinkers and determine phases by XRD and overall composition by XRF as shown in next sections.

3.1.2 XRD of clinkers and their interstitials

The XRD profiles of the clinkers and their "interstitials" of clinkers α, β, γ and δ are shown in Figures 6/7, 8/9, 10/11 and 12/13, respectively. In the extraction process the silicate phases C_3S and C_2S are removed, and the remaining phases are the "interstitials" usually used for C_3A and C_4AF, but here also including insoluble phases like calcium sulphates, magnesium oxide etc.

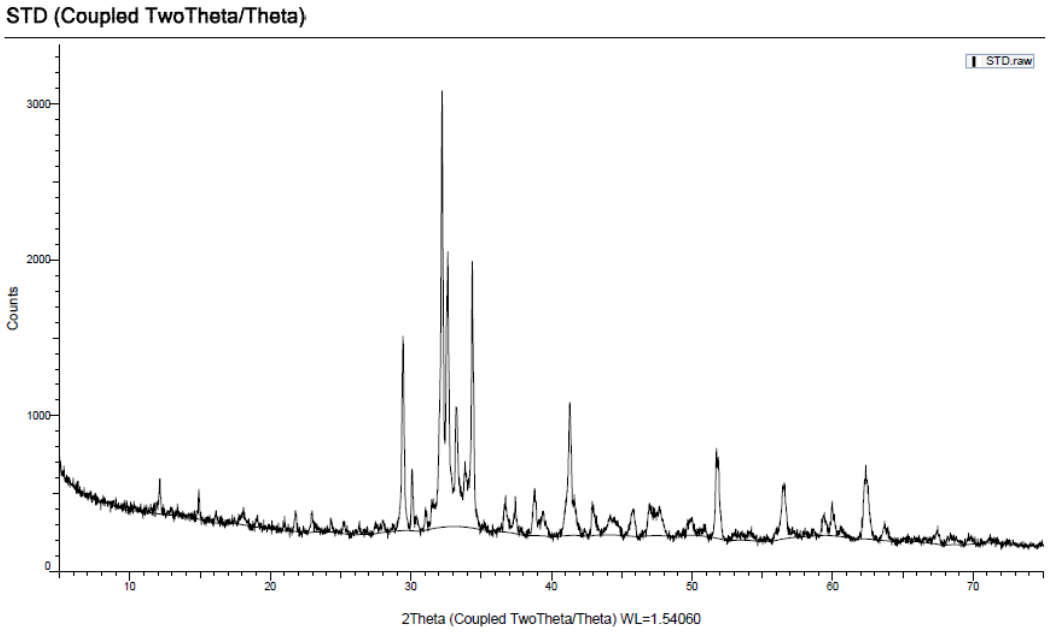

Figure 6: XRD profile of clinker α before extraction procedure

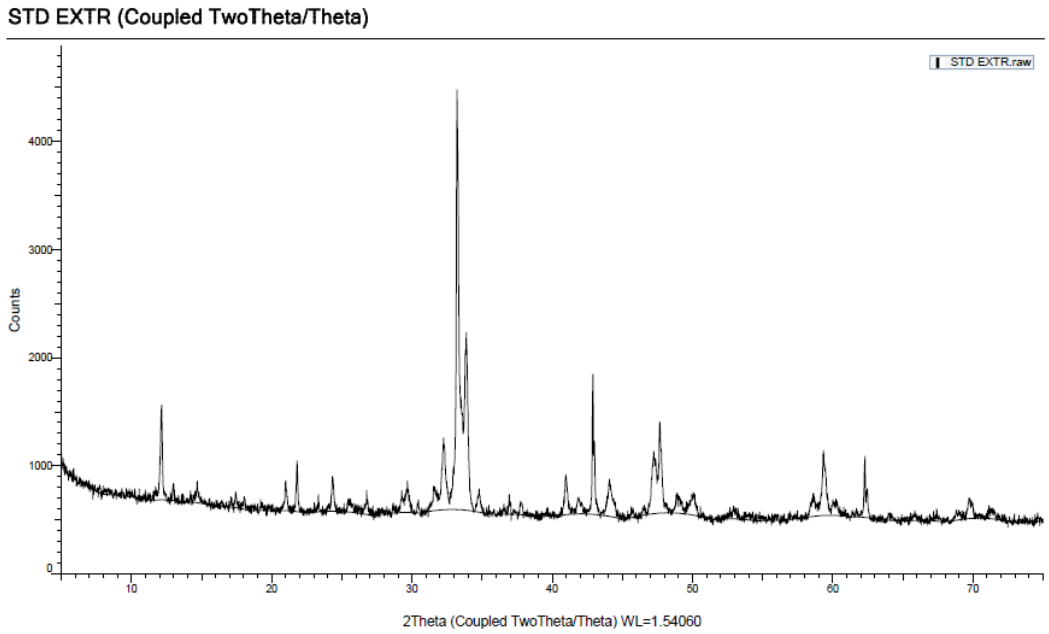

Figure 7: XRD profile of clinker α interstitials after extraction procedure

According to the Rietveld analysis of the clinker α XRD profile (like the one in Fig. 6) performed at Heidelberg Technology centre (HTC), the total C_3A content of 10% is distributed between 6.9% cubic and 3.1% orthorhombic modifications. The amount of C_4AF is also rather high with 10.2%, which can be seen from the complexity of peaks in the range 32-35° 2θ.

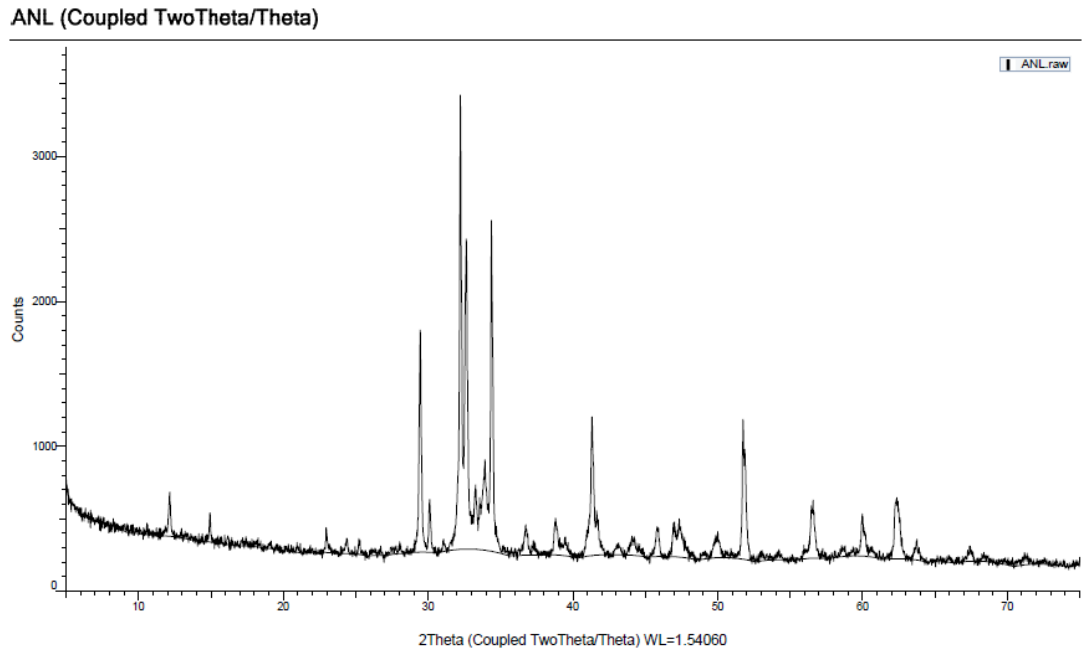

Figure 8: XRD profile of clinker β before extraction procedure

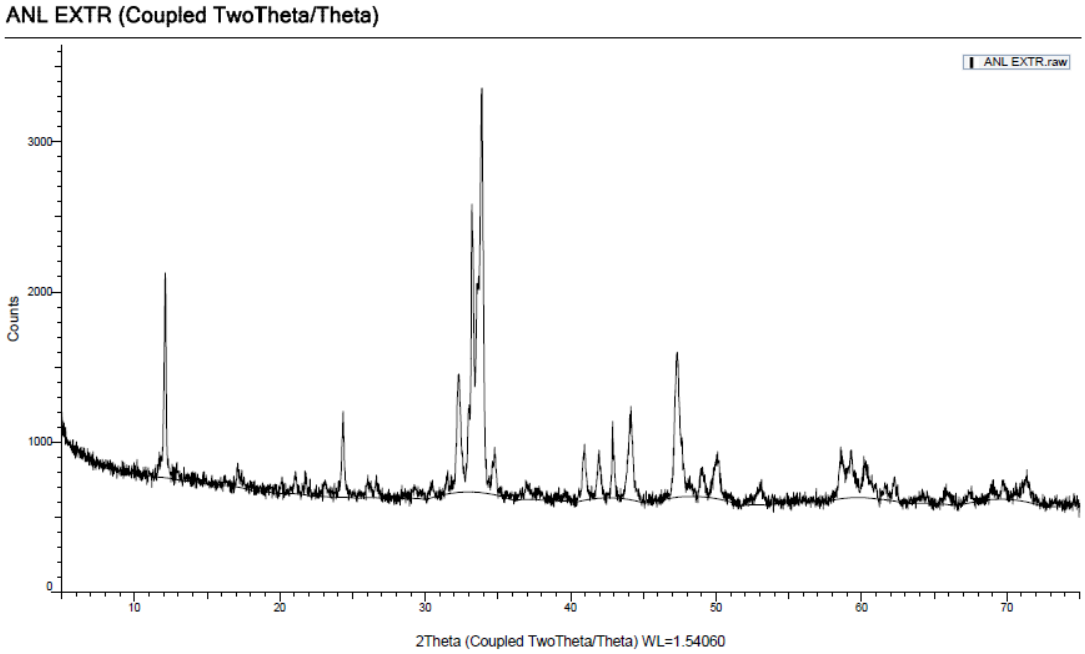

Figure 9: XRD profile of clinker β interstitials after extraction procedure

According to the Rietveld analysis of the clinker β XRD profile (like the one in Fig. 8) performed at Heidelberg Technology centre (HTC), the total C_3A content of 4.6% is distributed between 1.7% cubic and 2.9% orthorhombic modifications. The amount of C_4AF is also high with 14.1%, which can be seen from the complexity of peaks in the range 32-35° 2θ.

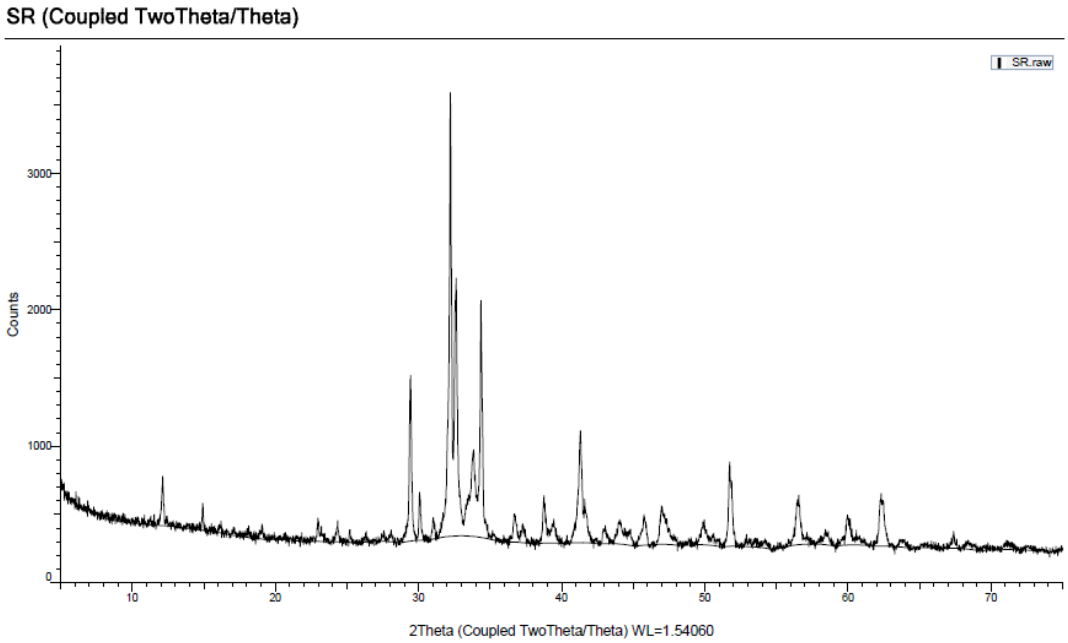

Figure 10: XRD profile of clinker γ before extraction procedure

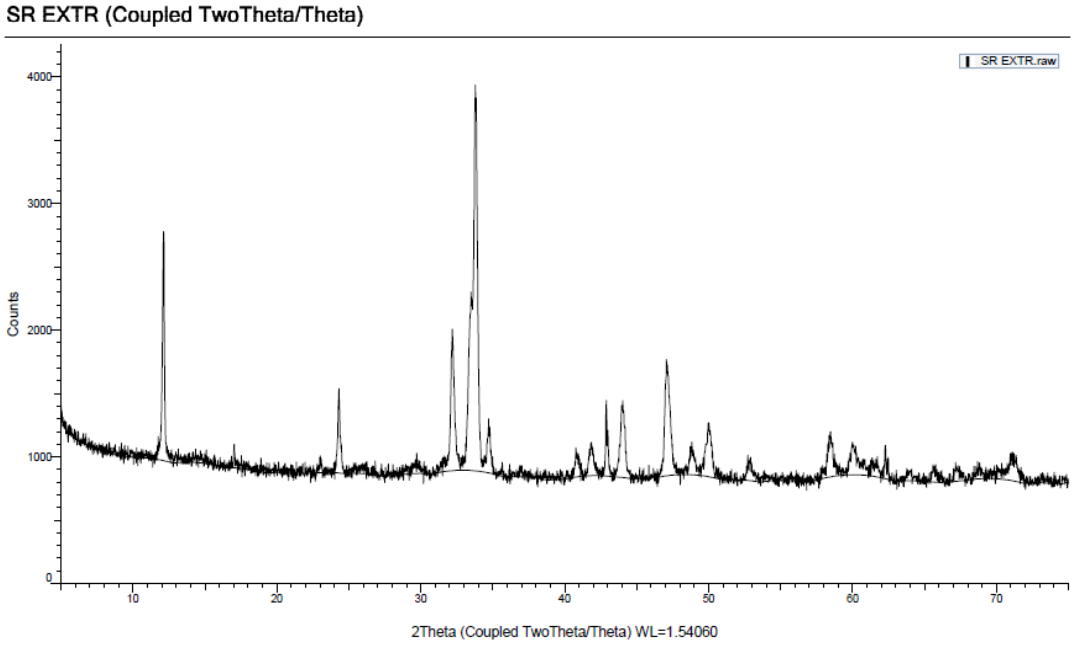

Figure 11: XRD profile of clinker γ interstitials after extraction procedure

According to the Rietveld analysis of the clinker γ XRD profile (like the one in Fig. 10) performed at Heidelberg Technology centre (HTC), the total C_3A content of 0.3% is distributed between 0.1% cubic and 0.2% orthorhombic modification. However, these are small amounts associated by high uncertainty and the major peaks overlaps with the cluster of major peaks in the range 32-35° 2θ from the 18.5% C_4AF.

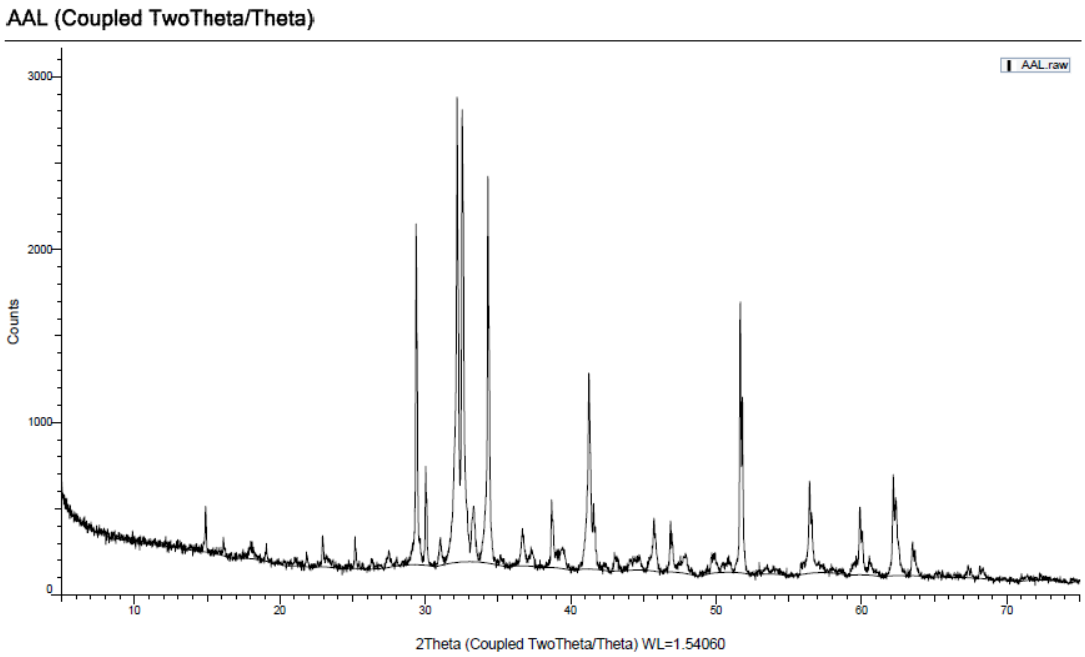

Fig. 12 XRD profile of clinker δ before the extraction process

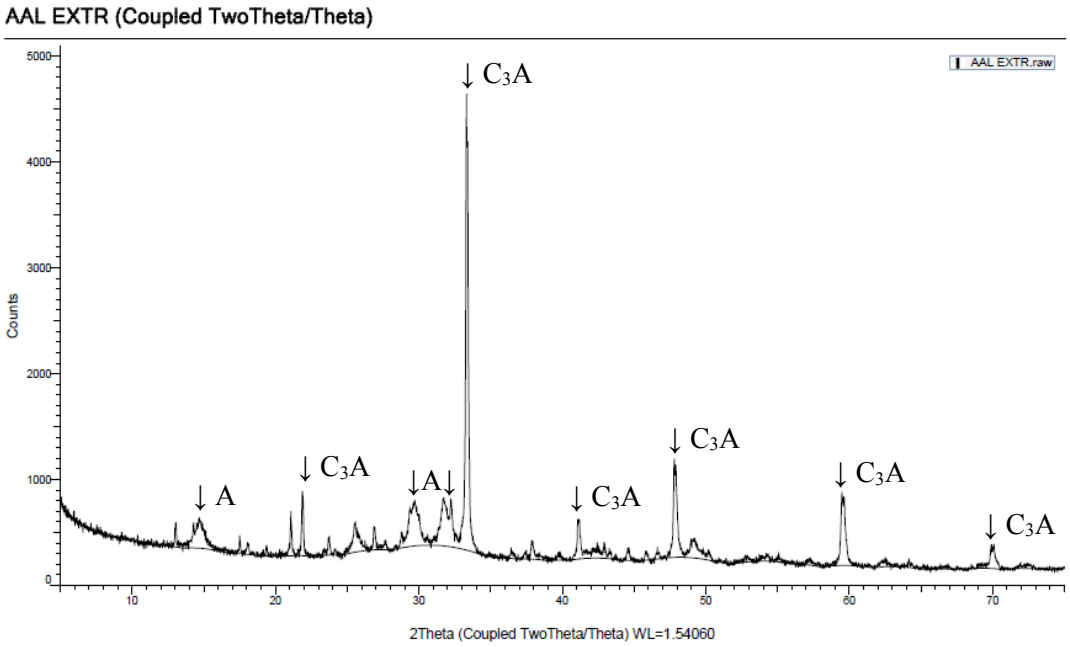

Fig. 13 XRD profile of "interstitials" from clinker δ after the extraction process. Peaks marked "A" are anhydrite.

In the XRD profile of interstitials in Fig. 13, in addition to C_3A and Anhydrite, there are possible very small amounts of Mayenite, $C_{12}A_7F_2$, and most certainly fluorellestadite, $Ca_{10}(SiO_4)_3(SO_4)_3F_2$, even its major peaks have partial overlap with anhydrite. This is a proof that anhydrite and possibly some fluoride were used as fluxes in the production of clinker δ. There is absolutely no trace of C_4AF as this phase would have given rise to a peak at about 12° 2θ as seen in for instance Fig. 11 for clinker γ that only contain C_4AF and no C_3A. According to the Rietveld analysis of the clinker δ XRD profile (like the one in Fig. 12) performed at Heidelberg Technology centre (HTC), the total C_3A content of 3.2% is distributed between 2.9% cubic and 0.3% orthorhombic modification, and the major peaks in Fig. 13 is indeed assigned to cubic C_3A. The 30.3% C_2S calculated from the Rietveld

analysis was solely of the β-modification, as opposed to the estimation of 16% belite from Bogue calculations. The higher "bump" in the background level at around 30° 2θ in Fig.13 compared to the interstitials of the other cements could be a sign of a higher content of an amorphous phase that might contain alumina.

3.1.3 ICP of clinker extraction liquid

The element compositions of the extraction liquid was measured by ICP to see if any of the clinkers had more or less alumina in their silicate phases as solid solutions and that presumably would enter the liquid phase. In particular is this interesting for clinker δ since its alumina content indicates a much higher C_3A content by a simple Bogue analysis (10.3%) than found by Rietveld analysis of XRD profiles (3.2%).

It is the first time organic solvents are used for ICP/MS and the solutions where thinned 500x with water. The content in original solution was in mg/kg solution; 14,980 Ca, 3,485 Si, 309 Al, 165 Mg and 9 S.

The density of the solution of 25 g maleic acid in 125 ml methanol (0.791 g/ml) and dissolved clinker had density 0.91 g/ml and a total mass of about 128.43 g taken into account the 8.9% residue in next section, meaning that the percentage of elements removed from 5 g clinker was 38.3% Ca, 8.91% Si, 0.79% Al and 0.42% Mg or as the respective oxides; 54.0% CaO, 19.2% SiO_2, 1.50% Al_2O_3 and 0.70% MgO.

The ratio between C_3S and C_2S *independently of solution density* can then be calculated from the calcium balance

$3 \cdot C_3S + 2 \cdot C_2S = 54.0\%$ Ca

And silicon balance

$C_3S + C_2S = 19.2\%$ Si

Giving $C_3S/C_2S = 15.6/3.6 =$ **4.3** while Rietveld (Table 2) says **2.10** and Bogue (Table 3) says **4.24**. Hence, it seems that there is something wrong with the given data from Rietveld in this case and that the simplified Bogue calculation is more correct.

The Rietveld analysis from HTC did not find any anhydrite, and the only sulphate phase found was 0.4% Arcanite, K_2SO_4 (corresponding to 0.18% SO_3) while the total SO_3 was 1.6% from CS-analysis. The XRD of interstitials for clinker δ showed the presence of anhydrite in Fig. 13.

3.1.4 XRF of extraction residue

Two parallel extractions of 5.012 and 5.008 g clinker δ gave residues of 0.452 and 0.440, respectively, or 8.9±0.2%. The XRD profile of interstitials in Fig. 13 revealed cubic C_3A and Anhydrite, with some fluorellestadite, $Ca_{10}(SiO_4)_3(SO_4)_3F_2$, as well as possibly very small amounts of Mayenite, $C_{12}A_7F_2$ (in this case F represents fluorine and not Fe_2O_3).

The oxide composition of the residue as measured by X-ray fluorescence (XRF) is listed in Table 8. The loss on ignition (LOI) to 1000 °C was 5.37% and the analysis was done on an ignited sample. The 15.3% SO_3 in the ignited found in Table 8 corresponds to 14.5% in the un-ignited sample and multiplying that with the fraction of residue gives an SO_3 content in the clinker of **1.3%** which is not far from the **1.6%** found by the CS analyser of HTC. This

corresponds quite well considering all the steps in the calculation involving individual uncertainties.

If one now make the assumption that all SiO_2 in the residue is in the form of fluorellestadite and is associated with 2 CaO on molar basis + 1 CaO associated with fluoride (not analysed) and all SO_3 is in the form of either fluorellestadite or anhydrite and is associated with 1 CaO (with the exception of 2K in Arcanite that holds one SO_3), one calculate a C/A molar ratio of 2.0 far from 3 in C_3A. If one only subtract for sulphate, one get C/A = 2.9 (close to C_3A) or if one do not subtract CaO from any of the other oxides C/A = 3.6.

Assuming that all Al_2O_3 in the residue is associated with C_3A and that the small amount of Al in the liquid from the extraction (1.50% Al_2O_3 of clinker) was associated with the alite (typical contaminants of C_3S in clinker are Mg and Al) or belite, one arrives at a C_3A content of the clinker of 5.5% C_3A. If one subtract 1.5% Al_2O_3 in the Bogue calculation belonging to C_3S/C_2S one end up with 6.3% C_3A. Thus, it is likely that the C_3A content is around 6% (about double of Rietveld analysis), but some of it may be in the form of "glass" not detectable by XRD due to its amorphous nature. There are signs of this in the diffractogram of Fig. 13 appearing as broad "bumps" on the base line. Also in Fig. 4 (image in the middle to the left) there are sign of two different aluminate phases with different C/A (analysis points D8 and D9 with composition in Table 6).

Table 8 The oxide composition of the ignited extraction residue of clinker δ

Oxide	Content (%)
CaO	48.7
Al_2O_3	24.7
SO_3	15.3
SiO_2	4.3
MgO	3.0
K_2O	1.8
Fe_2O_3	1.2
TiO_2	0.4
Sum	99.4

3.1.5 Potential reasons for higher strength of δ clinker compared to the other clinkers

The reason for the higher strength of cement made from the δ clinker compared to the others is several;

- It contains more calcium sulphate than the others as anhydrite is used as a flux in the production of the clinker (about 1.5% anhydrite of clinker mass).
- It contains about the double amount (≈ 6%) of crystalline and possibly amorphous C_3A than predicted by the Rietveld analysis of XRD.
- If the other clinkers haves been "under-sulphated" by the addition of 3% gypsum, the clinker δ has got sufficient calcium sulphate not only to form early ettringite, but to let the excess accelerate C_3S hydration.
- The C_3S content is much higher for δ (63.6%) than for α (49.1%) clinker which contributes to the higher 1 day strength in Fig. 2, even though the fineness is only marginally higher.
- The seemingly better response to blending with limestone for the δ clinker than for the other clinkers after 28 days curing (Fig. 1) also support a higher content of C_3A than predicted by the Rietveld analysis considering the formation of calcium monocarbo-aluminate hydrate and stabilization of ettringite leading to more water bound as hydrates.

3.2 Investigation of microstructure of mortar

3.2.1 Selection of mortar samples

The mixes in Table 9 were taken from mortar prisms which had been stored at 20°C submerged in saturated lime solution for 28 days. After 28 days a slice of the prisms was sawn off and crushed. The resulting pieces were stored in ethanol until polished samples could be prepared.

Table 9: Samples analysed with SEM-WDS

sample name	Material	Trivial name
mix 45	65% β clinker + 30% C FA + 5% limestone	ANL + LN21
mix 47	65% β clinker + 30% D FA + 5% limestone	ANL + STEAG
mix 63	65% δ clinker + 30% C FA + 5% limestone	AAL + LN21

The mixes 45, 47 and 63 were chosen for the following reasons:
- clinker δ resulted in a considerable higher strength than clinker β (see Fig. 1)
- the strength increase observed when replacing 5% C fly ash with 5% limestone powder is relatively seen larger for the β clinker than the δ clinker (see Fig. 14)
- the strength increase observed when replacing 5% C fly ash with 5% limestone powder is low for all the clinkers (see Fig. 14).

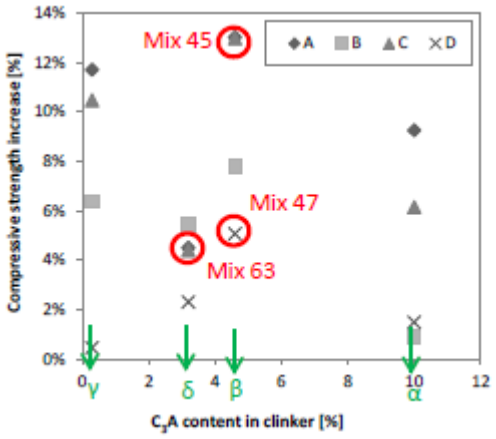

Fig. 14 Compressive strength increase when replacing 5% fly ash with 5% limestone powder

The fly ash D gave higher strength compared with any other of the fly ashes in combination with for instance clinker δ as shown in Fig. 3.

3.2.2 Microstructure of the mortar samples

Fig. 15 shows and overview of the microstructure of the samples at 250x and 1000x magnification respectively. A closer look at sample 47 is shown in Fig. 16 with a number of points at details suspected to be AFm or AFt phases. The elemental compositions of these selected points are given in Table 10 and corresponding compounds in Table 11. More detailed images of the microstructure of mortar samples 45, 63 and 47 are given in Figures 17/18, 19/20 and 21/22/23, respectively. These micrographs are further used for point analyses as indicated.

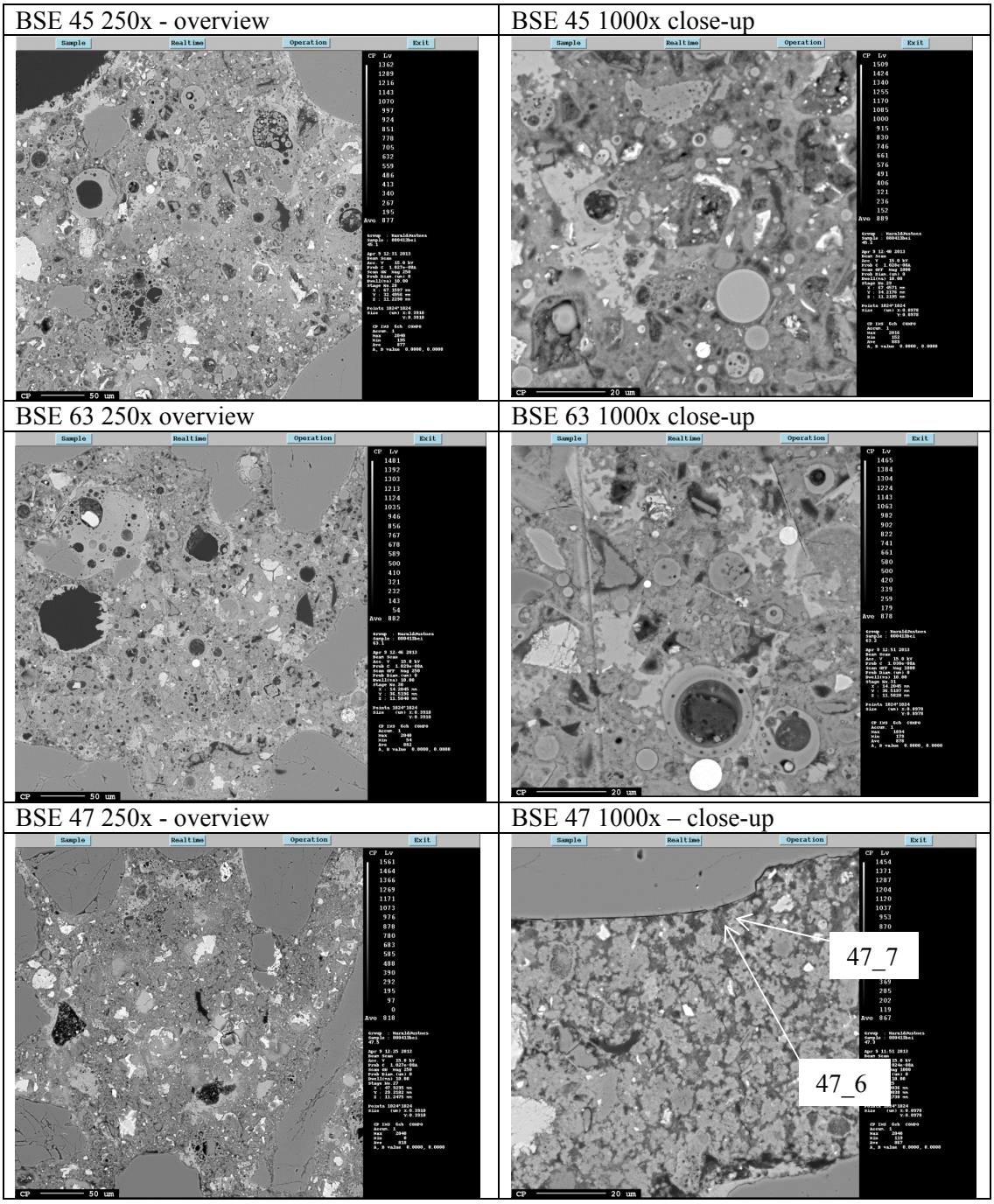

Fig. 15 Overview of the microstructure of samples 45, 63 and 47 at 250x (left column) and 1000x (right column) magnification. The composition of the analysis points 47_6 (dark grey matter) 47_7 (light grey matter) is given in Table 10.

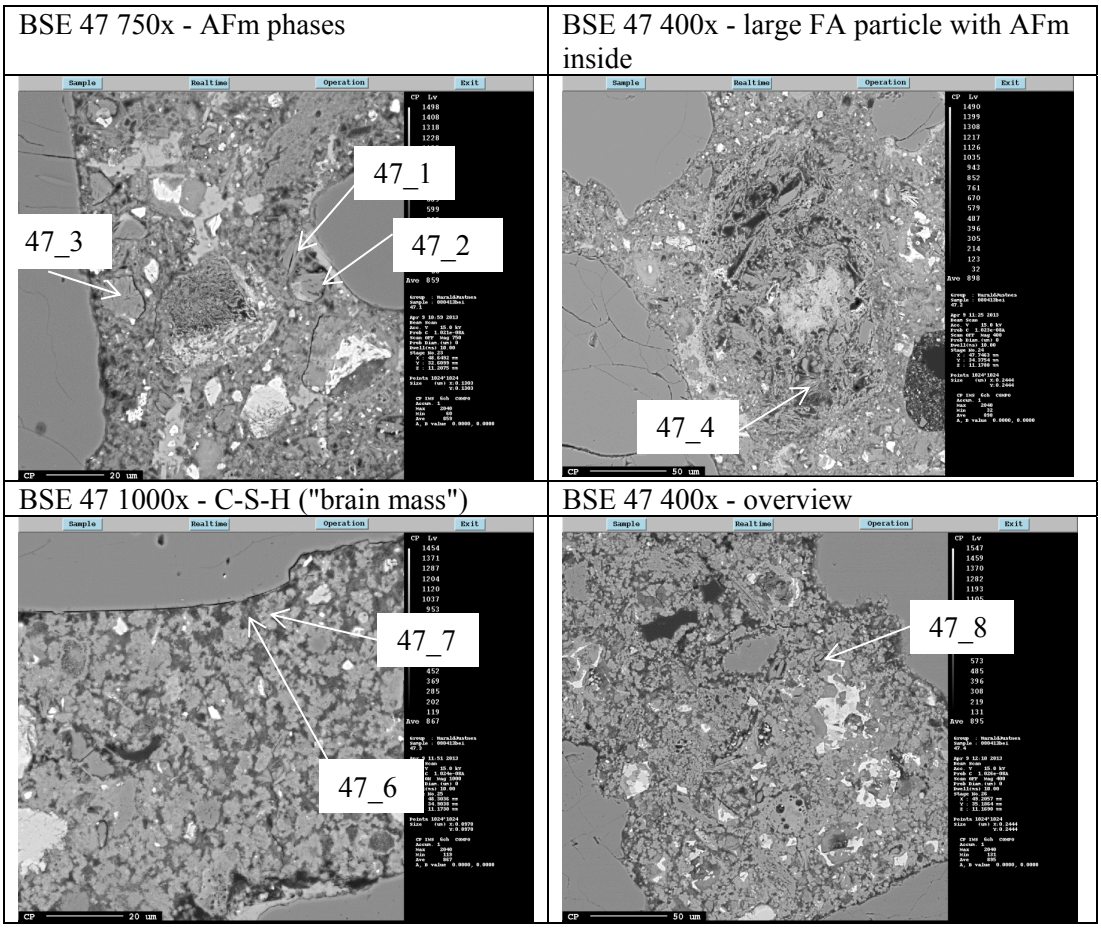

Fig. 16 A closer look at sample 47 with a number of points for wave length dispersive analysis of X-rays (WDX). The compositions of these points are given in Table 10.

Table 10 Element composition (atom%) of points in Figure 16.

Point	Na	O	Fe	K	Mg	F	Ca	Si	Al	S
47_1	0.00	69.56	0.15	0.02	0.35	0.04	18.07	0.87	10.0	0.93
47_2	0.02	70.04	1.41	0.01	0.33	0.00	17.52	1.01	8.53	1.12
47_3	0.00	70.82	0.41	0.01	0.26	0.00	17.71	0.49	9.38	0.92
47_4	0.05	66.68	0.09	0.06	0.03	0.11	20.67	0.33	5.72	6.30
47_6	0.42	53.72	1.08	0.35	1.08	0.00	26.74	6.70	5.37	4.54
47_7	0.24	61.30	0.59	0.40	0.55	0.00	24.74	7.40	3.40	1.38
47_8	0.06	60.53	1.37	0.04	0.16	0.00	22.82	0.50	12.00	2.54

Table 11 Interpretation of compounds complying with analysis in Table 10

Point	Ca/Al	S/Al	Si/Al	Interpretation
47_1	≈2	≈0.1	≈0.1	hydroxy or carbonate AFm
47_2	≈2	≈0.1	≈0.1	hydroxy or carbonate AFm
47_3	≈2	≈0.1	≈0.1	hydroxy or carbonate AFm
47_4	≈4	≈1	≈0.1	50/50 Sulphate/Carbonate AFm
47_6	≈4	≈1	≈1	dark grey S rich CASH
47_7	≈7	≈0.4	≈2	light grey CASH, less S
47_8	≈2	≈0.2	≈0.1	hydroxy or carbonate AFm

45 (ANL+LN21) BSE1 scale 50 um

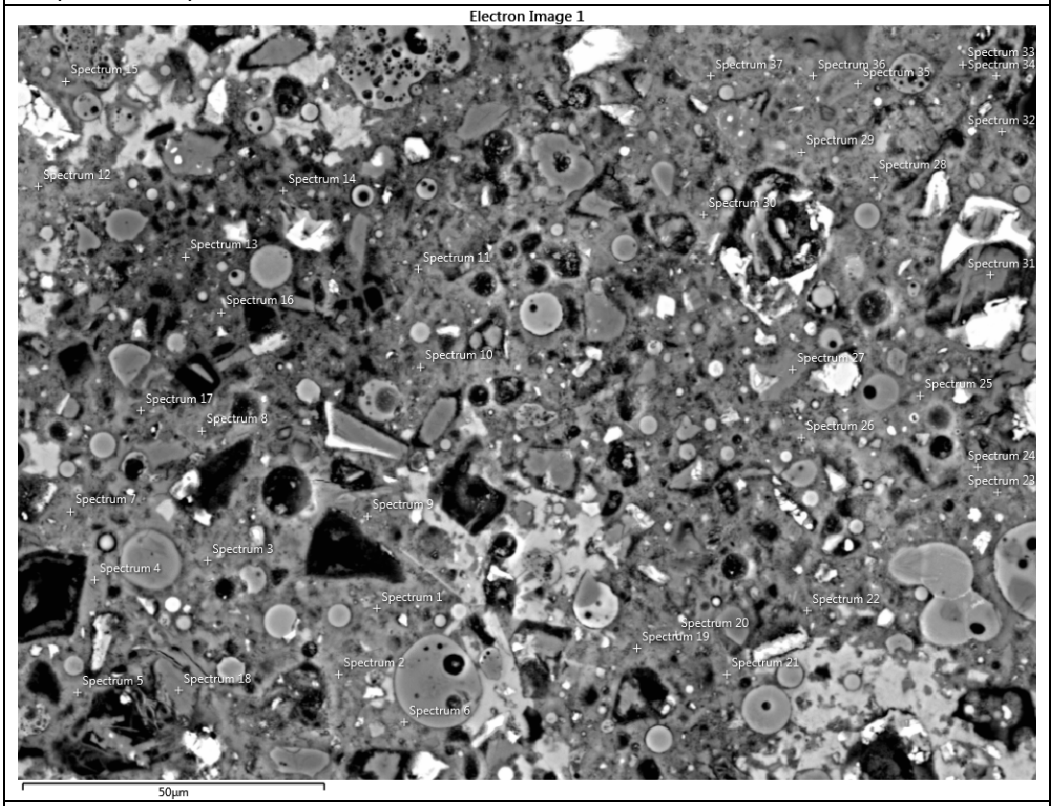

45 (ANL+LN21) BSE2 scale 50 um

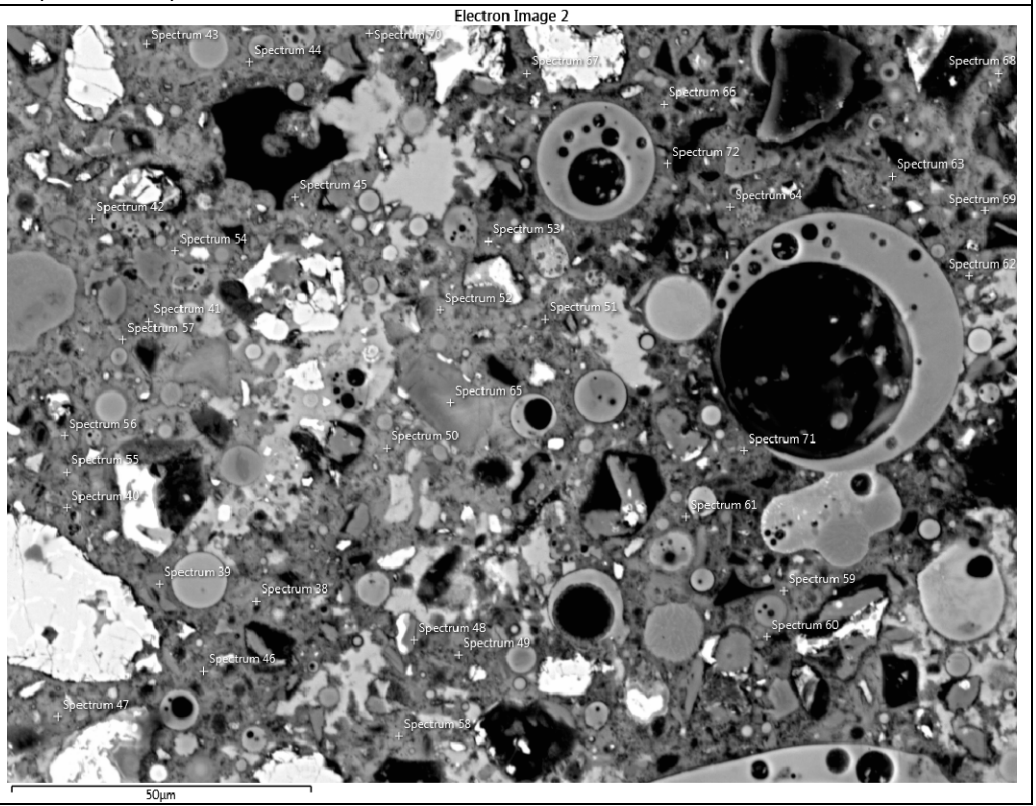

Fig. 17 Microstructure of mortar sample 45; 65% β clinker + 30% FA C + 5% limestone

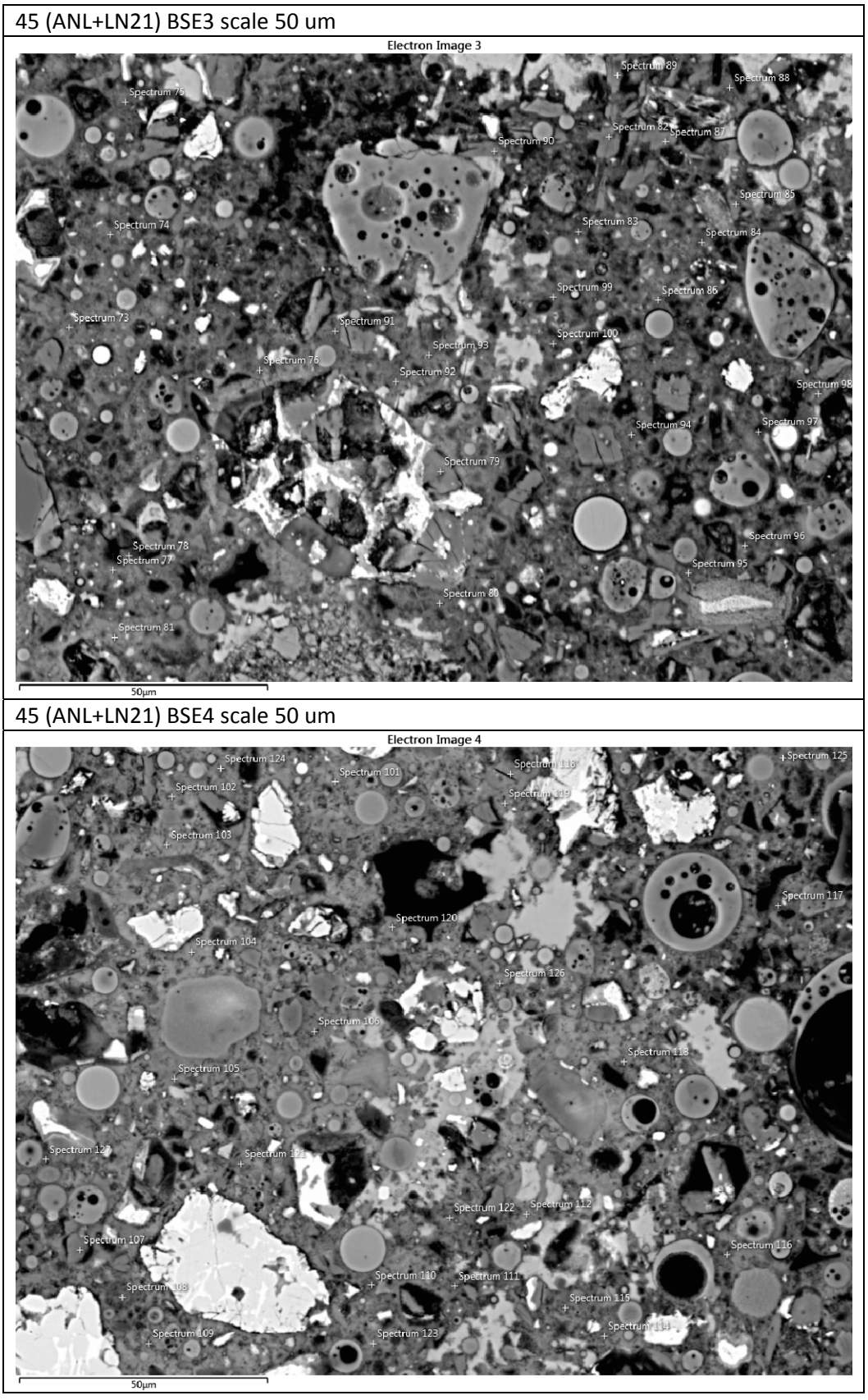

Fig. 18 Microstructure of mortar sample 45; 65% β clinker + 30% FA C + 5% limestone

63 (AAL+LN21) BSE1 scale 50 um

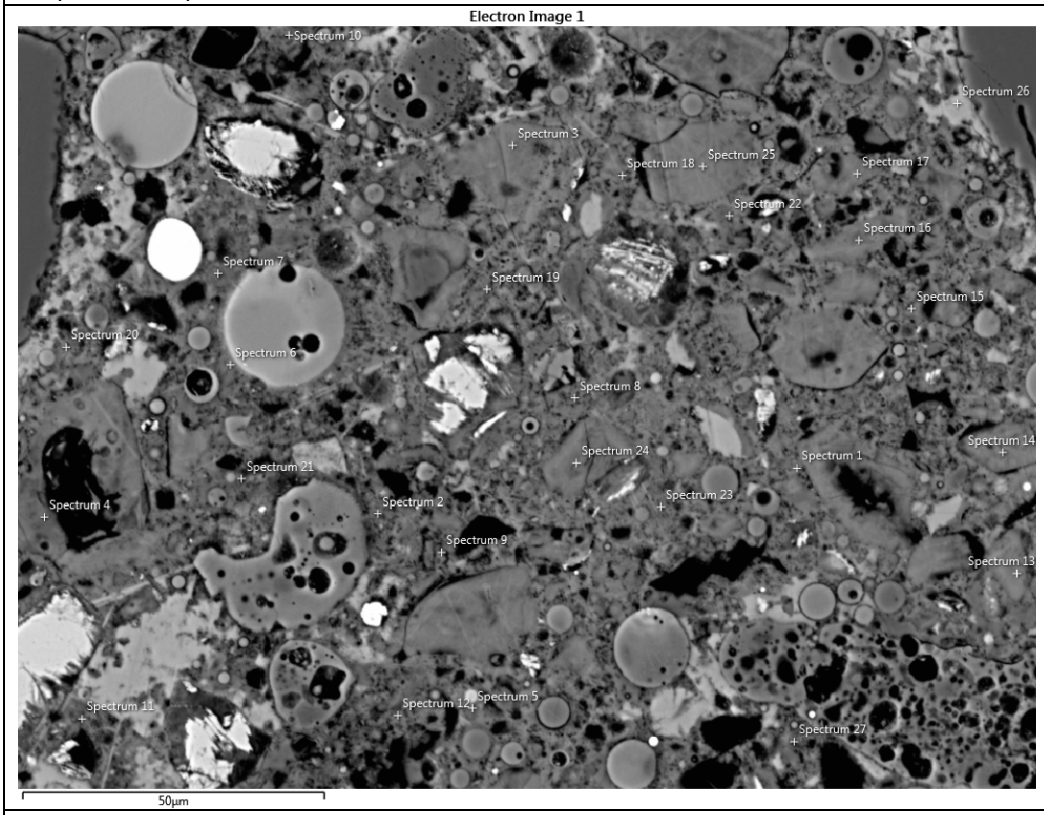

63 (AAL+LN21) BSE2 scale 50 um

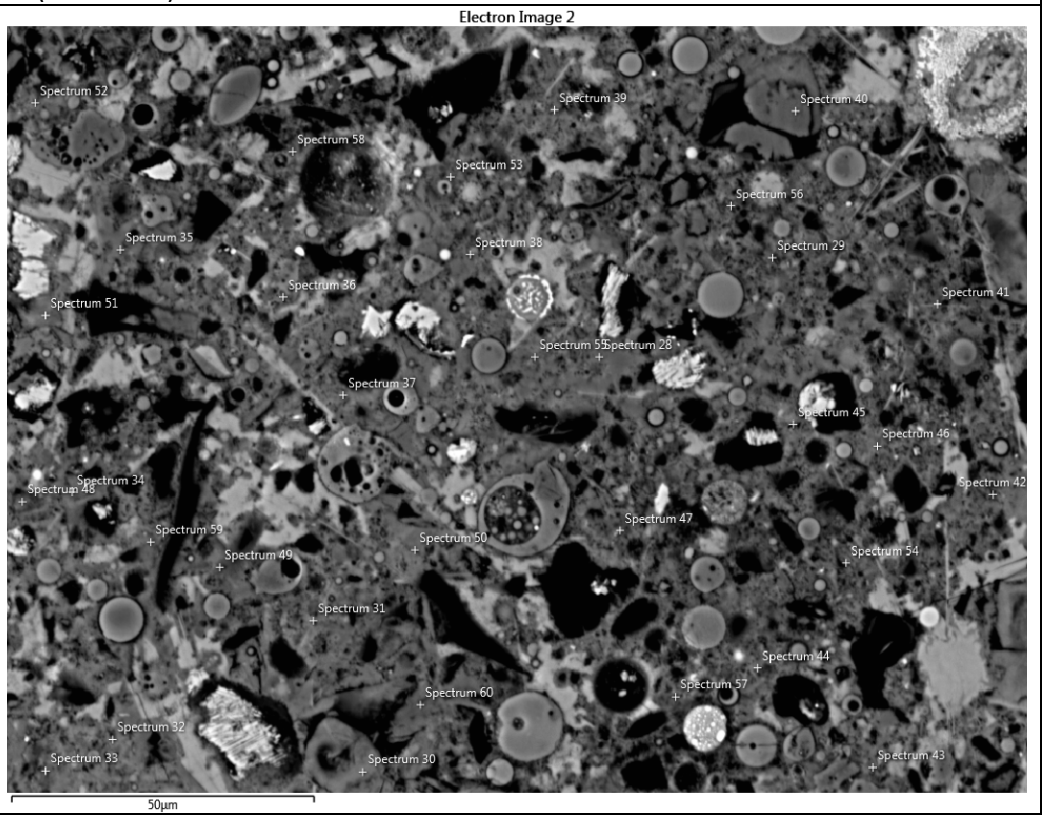

Figure 19 Microstructure of mortar sample 63; 65% δ clinker + 30% FA C + 5% limestone

63 (AAL+LN21) BSE3 scale 50 um

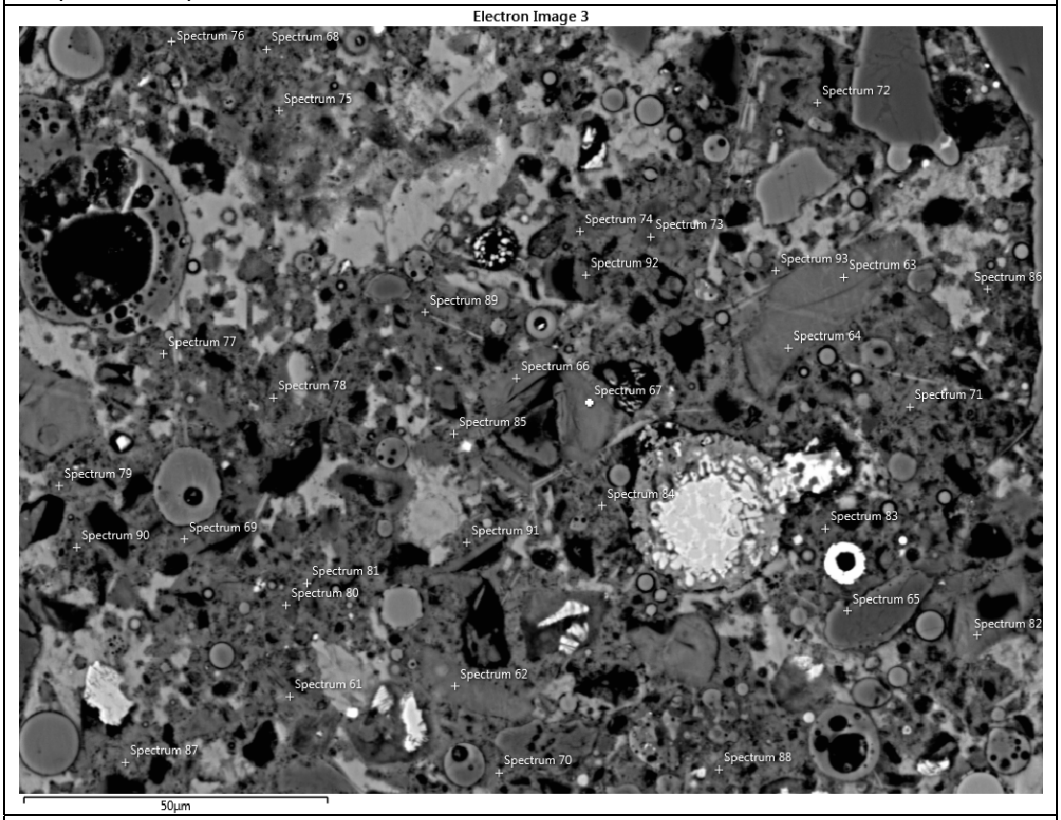

63 (AAL+LN21) BSE4 scale 50 um

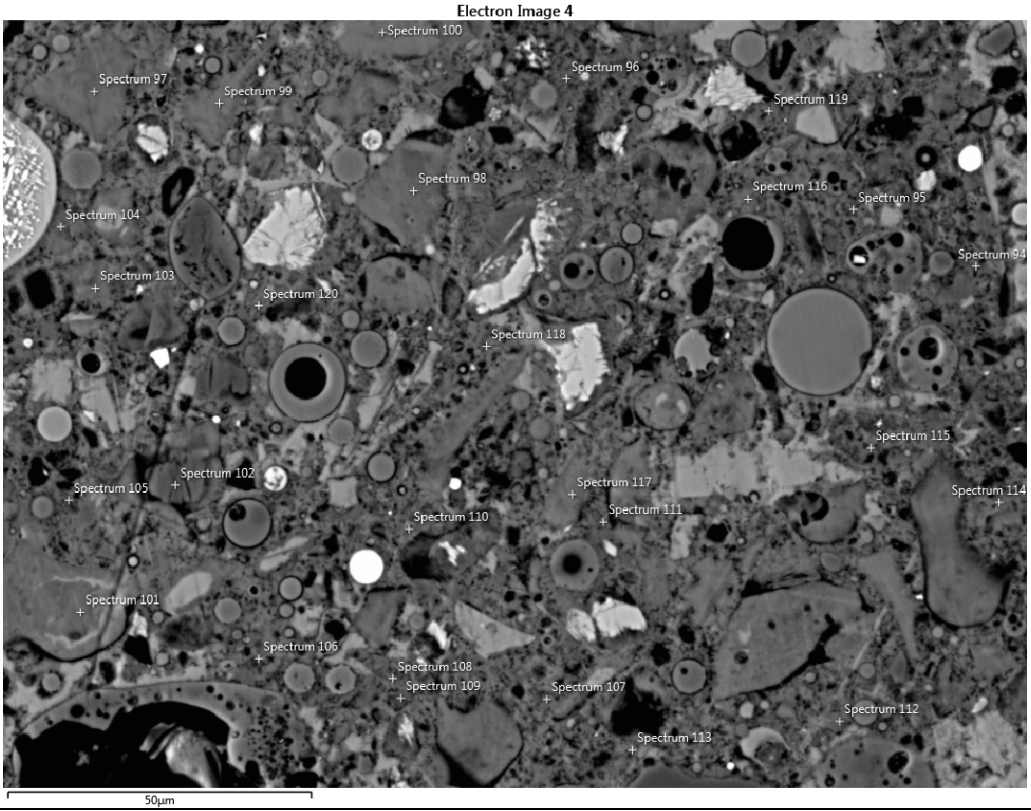

Fig. 20 Microstructure of mortar sample 63; 65% δ clinker + 30% FA C + 5% limestone

47 (ANL+STEAG) BSE1 scale 50 um

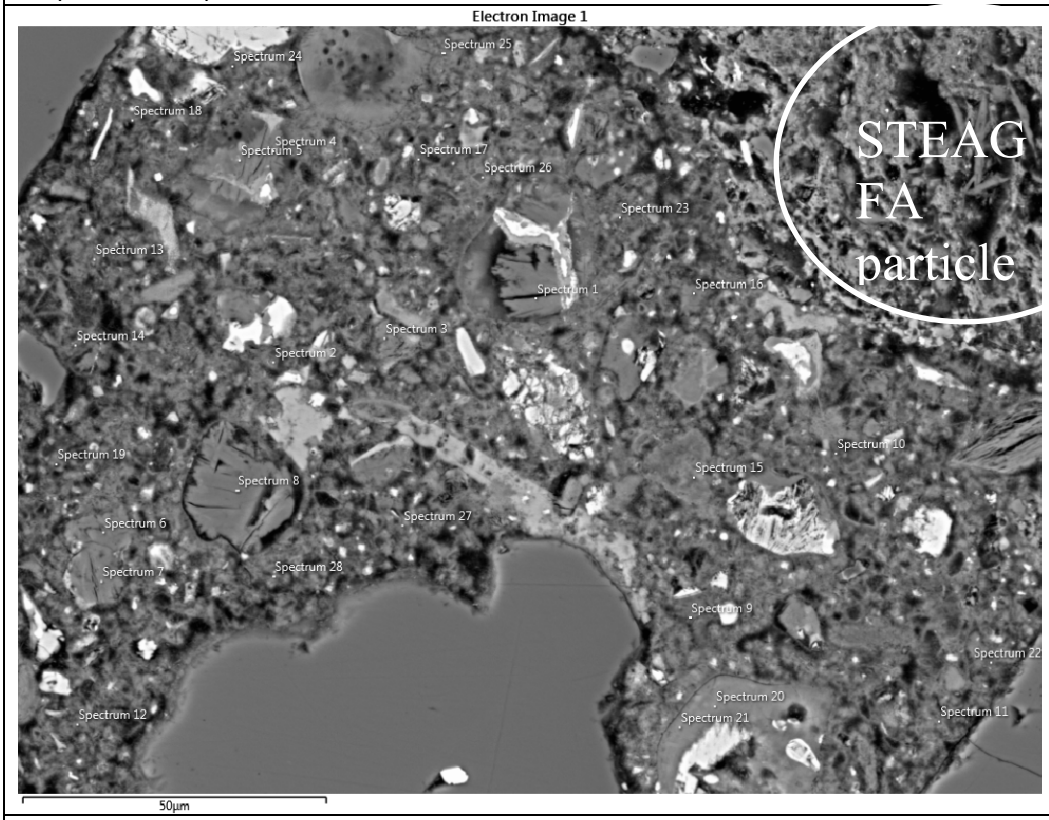

47 (ANL+STEAG) BSE2 scale 50 um

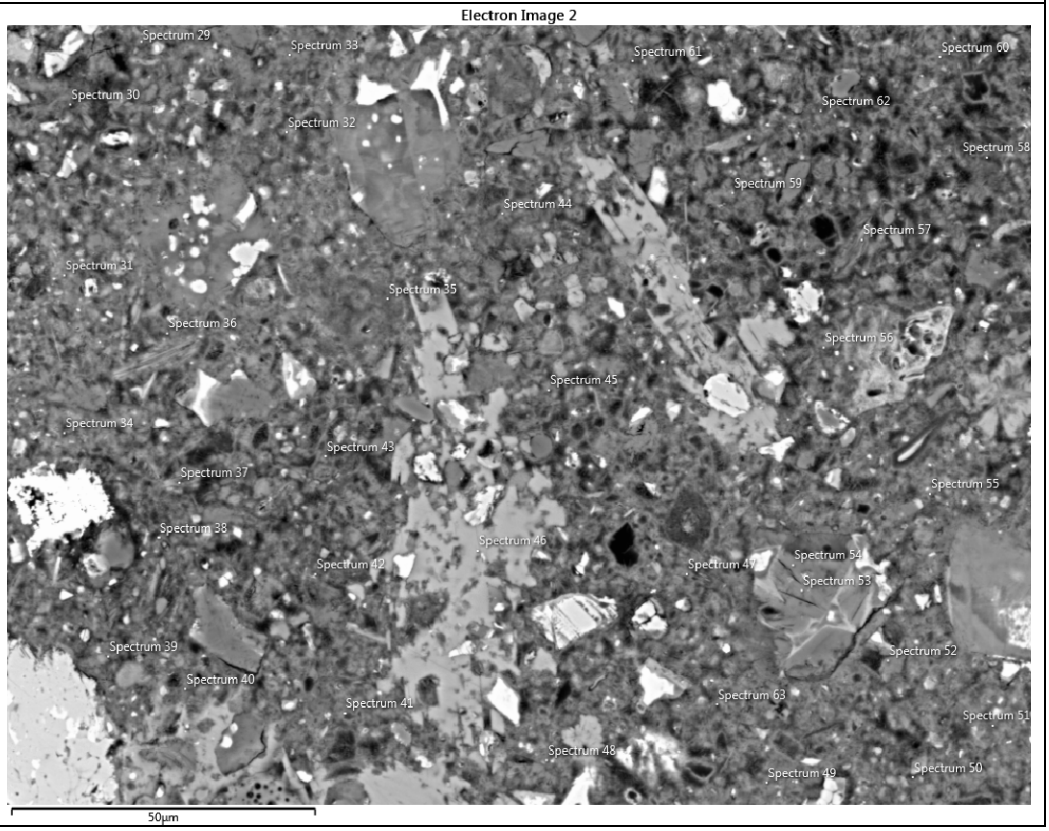

Figure 21 Microstructure of mortar sample 47; 65% β clinker + 30% FA D + 5% limestone

47 (ANL+STEAG) BSE3 scale 50 um

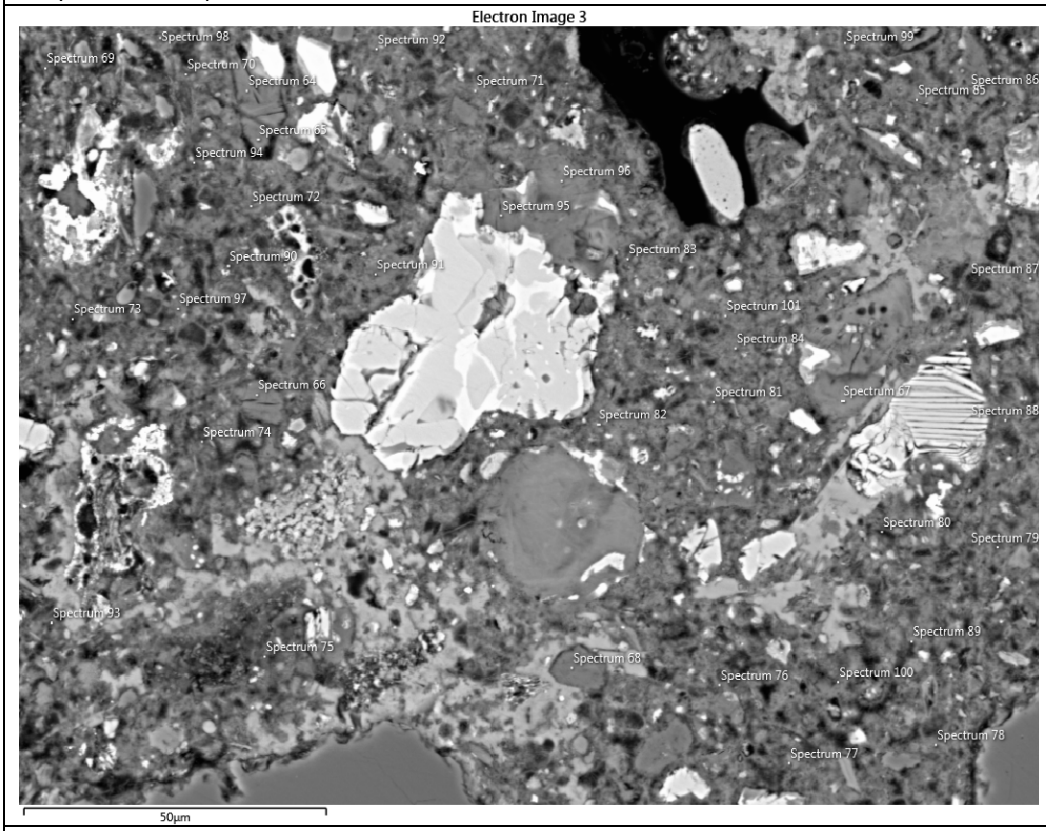

47 (ANL+STEAG) BSE4 scale 50 um

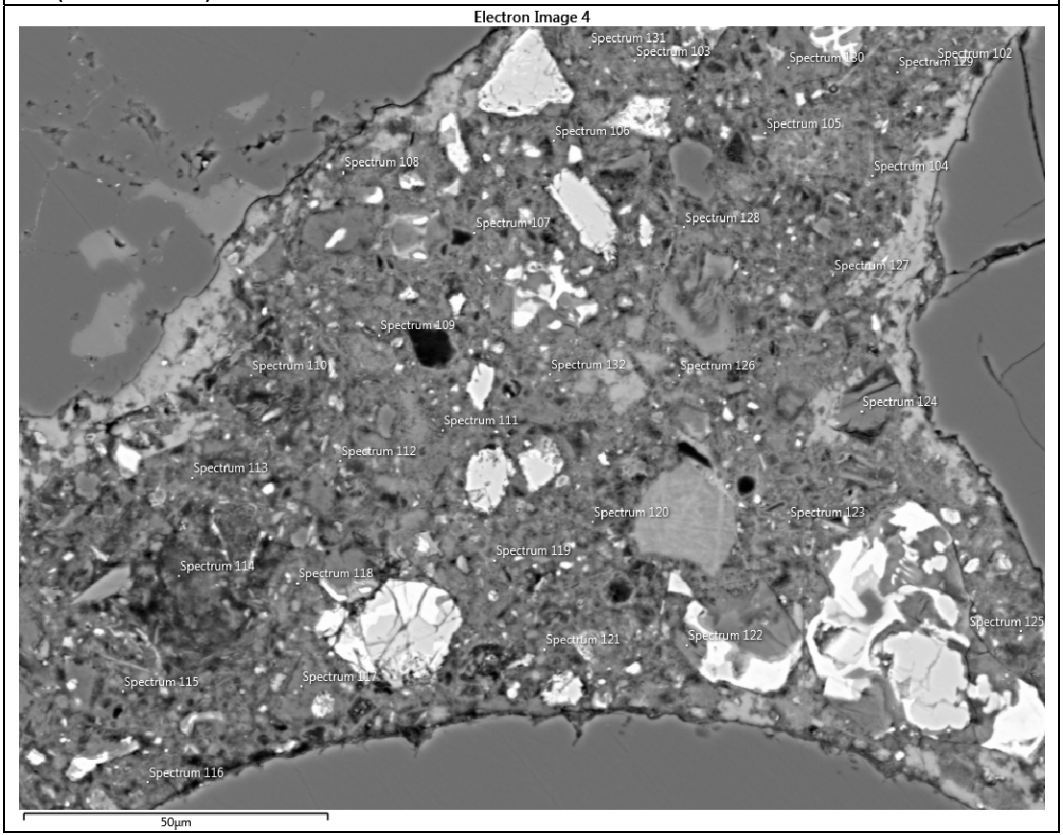

Figure 22 Microstructure of mortar sample 47; 65% β clinker + 30% FA D + 5% limestone

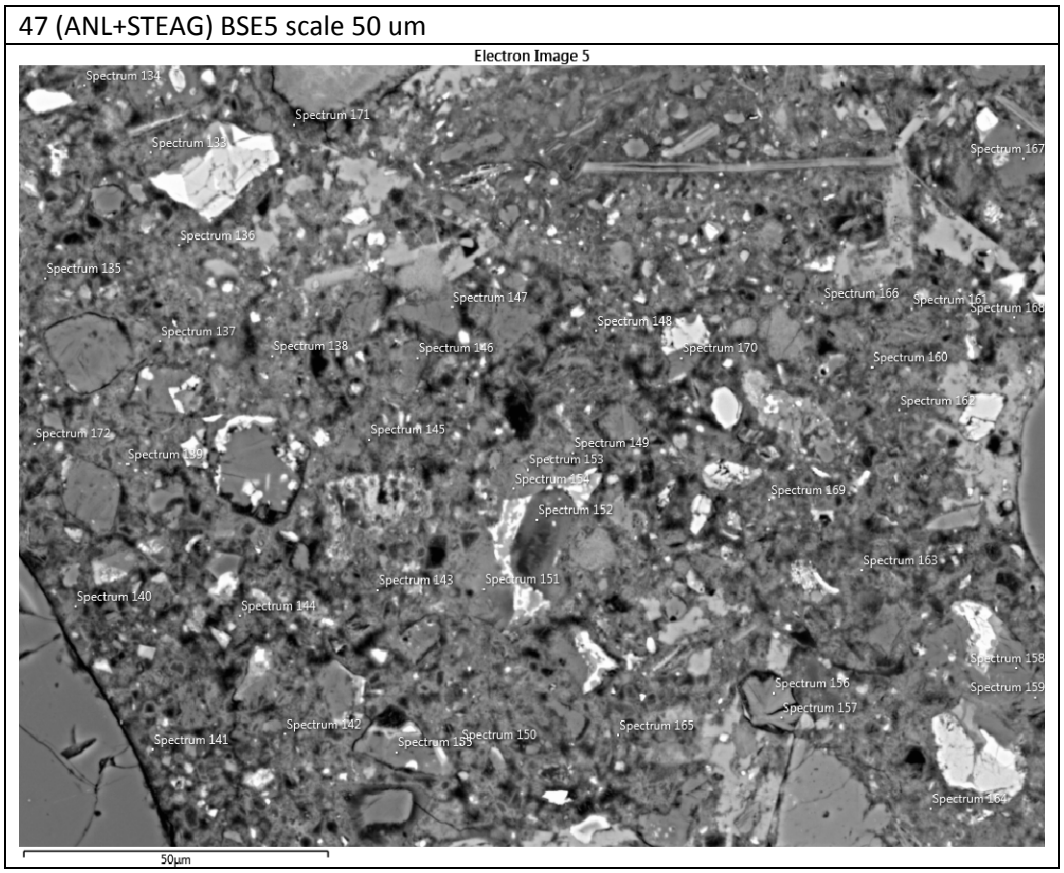

Figure 23 Microstructure of mortar sample 47; 65% β clinker + 30% FA D + 5% limestone

The general observations from Figures 17-23 is that

1. All mortars contain ample calcium hydroxide for further pozzolanic reaction
2. There is more unreacted cement grains in mortar with clinker β than with clinker δ, but this is mostly unreacted C_4AF (the least reactive phase) that is not present in clinker δ.
3. Fly ash C consist of the classical alumina-silicate glass spheres still present as unreacted particles embedded in the matrix, while what is left of fly ash D is irregular particles with quite an open structure seen from new crystals growing inside it.
4. There is a tendency of more pores filled with AFt/AFm phases when fly ash D is employed that can be due to its much higher sulphate content and potential higher reactivity due to its less glassy nature and more open structure.

3.2.3 EDS point analyses

During a SEM-EDS point analysis the elemental composition of the volume of approx. 1 um is analyzed. This volume can comprise a mixture of different phases. In order to interpret EDS point analysis results, the elemental ratios in that point are calculated and they are plotted in a graph together with the ideal composition of typical cement hydration phases. If a point contains a mixture of phases it will be positioned in between the points indicating the ideal composition of these phases. The advantage of SEM-EDS compared to e.g. XRD is that the phases do not need to be crystalline. Therefore, the chemical composition of the main hydration phase of Portland cement, C-S-H, which is X-ray amorphous can be analyzed with this technique.

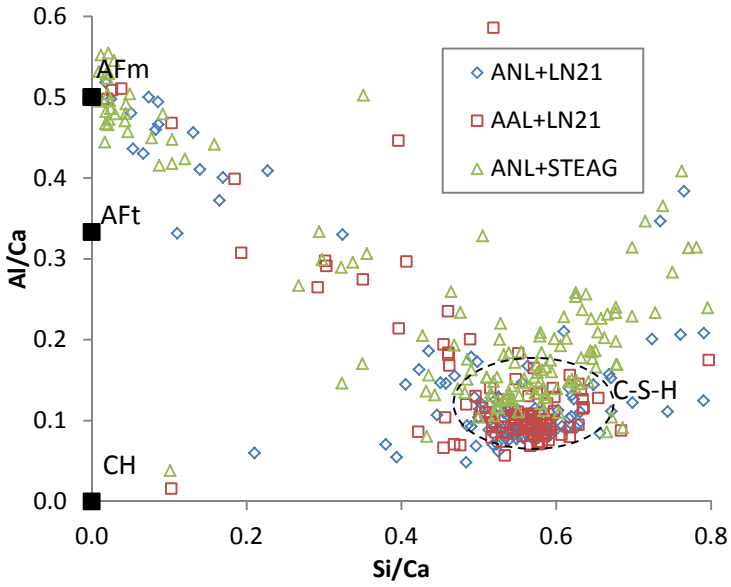

Figure 24: Al/Ca ration as function of Si/Ca ratio of the EDS point analyses of the different blended cements tested. This graph serves to indentify the Ca/Si ration of the C-S-H and the aluminate uptake of the C-S-H as Al/Ca. In addition AFm and AFt phases can be distinguished. Points from matrix of mortars 45, 63 and 47 are plotted here as diamond, square and triangles, respectively.

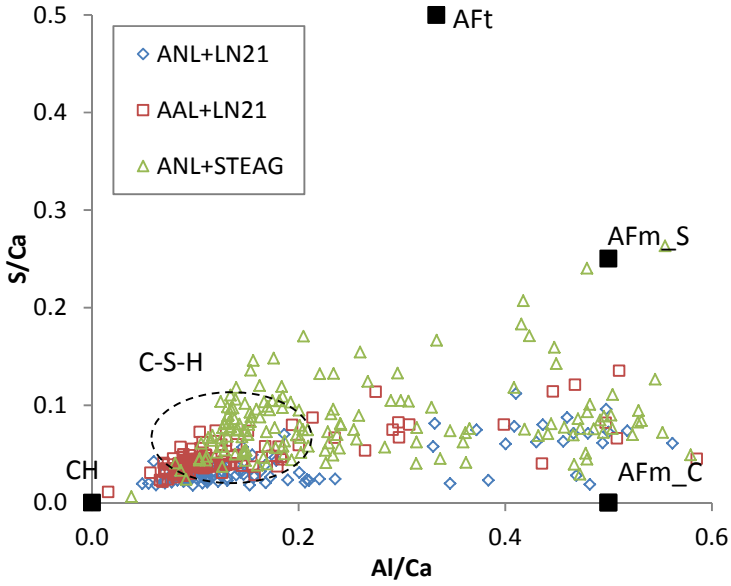

Figure 25: S/Ca ration as function of Al/Ca ratio of the EDS point analyses of the different blended cements tested. This graph serves to indentify the sulphate containing AFm and AFt phases (AFt = ettringite, AFm_S = monosulphoaluminate and AFm_C = monocarboaluminate). Points from matrix of mortars 45, 63 and 47 are plotted here as diamond, square and triangles, respectively.

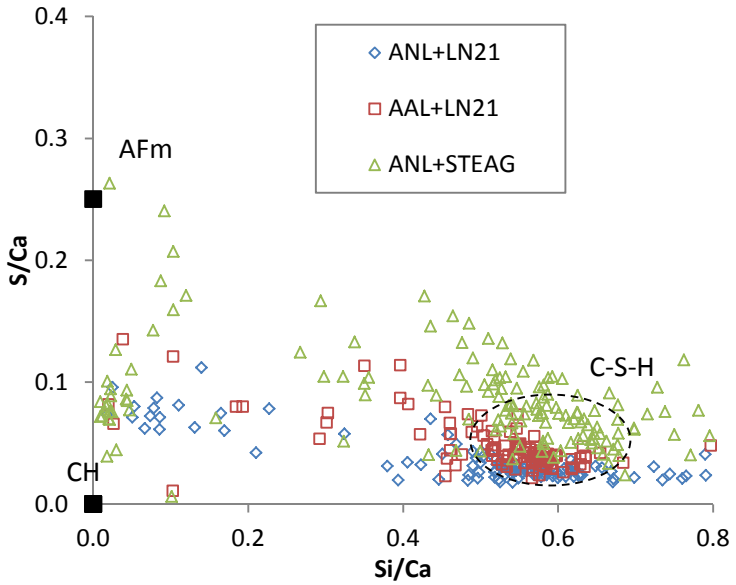

Figure 26: S/Ca ration as function of Si/Ca ratio of the EDS point analyses of the different blended cements tested. This graph serves to indentify the Si/Ca ratio of the C-S-H and the sulphate uptake in the C-S-H. AFm represents monosulphate in this graph. Points from matrix of mortars 45, 63 and 47 are plotted here as diamond, square and triangles, respectively.

From Fig. 24**Figure** and 26 the composition of the C-S-H in the different tested mixes can be determined. In Table 12 the elemental ratios of the C-S-H phase are given. It should be noted that C-S-H is a heterogeneous phase. The ratios reported in Table 12 should therefore be interpreted with care. Some clear trends regarding the C-S-H in the different tested mixes can however still be detected:

- *clinker type – mortar 45 vs. 63 (β vs. δ clinker with FA C):*
  - no significant difference in Al/Ca and Si/Ca ratio depending on the clinker type
  - slightly higher S uptake in the C-S-H for clinker δ, probably because it contain more calcium sulphate since anhydrite was used as flux
- *fly ash type – mortar 45 vs. 47 (FA C vs. FA D in clinker β)*
  - Fly ash D results in a significantly higher Al/Ca ratio, hence higher aluminate uptake in the C-S-H compared to Fly ash C. The Ca/Si ratio stays however similar. The glass composition of FA D contains most Al_2O_3 (see Table 5)
  - Fly ash D results in a significantly higher S uptake in the C-S-H compared to fly ash C, probably in contains much more sulphate (6.6.% SO_3) than the other (0.2 % SO_3) as seen from Table 4.

Table 12: The composition of the C-S-H phase in the different mortars

Approx. composition C-S-H	**45:** β+FA C	**63:** δ+FA C	**47:** β+FA D
Si/Ca	0.63	0.63	0.68
Al/Ca	0.09	0.08	0.15
S/Ca	0.25	0.30	0.50

In Fig. 25 and 26, the AFt and AFm phases present in the different test mixes can be identified. All mixes contain monocarboaluminate (AFm_C) and monosulphoaluminate (AFm_S). In contrast to the other mixes the 47: β+FA D mix seem to contain ettringite finely intermixed with the C-S-H caused by the higher sulphate content.

3.2.4 Findings from microstructure of mortar

In the introduction the reason for choosing the mixes 45, 47 and 63 was given by posing the following three research questions:

1. Q: Clinker δ (AAL) resulted in a considerable higher strength than clinker β (ANL)

   A: From the BSE images a greater degree of reaction was observed for δ compared to β clinker. The latter clinker has also a high content of C_4AF (14.1%) that has not reacted much. This might explain the higher strength. See also section 3.1.5.

2. Q: The strength increase observed when replacing 5% C fly ash (LN21) with 5% limestone powder is relatively larger for the β clinker (ANL) than the δ clinker (AAL) (see Fig. 14)

   A: SEM-EDS indicated that the phases formed in both blends (β + FA C vs. δ + FA C) are similar. The clinker type does not appear to affect the type of phases formed. Hence the difference in strength increase can only be explained by differences in the quantity of the phases formed.
   If clinker δ has reacted more, more C-S-H is expected to form. C-S-H incorporates Al and therefore less Al might be available to form AFm and AFt phases and this might lead to a reduction of the synergetic effect.
   Cement based on clinker δ also contain more calcium sulphate as anhydrite is used as flux, thus there is more AFt relative to AFm phase making less AFm able to react with limestone. Aft is stable in contact with limestone.
   However, in the β clinker mix unreacted C_4AF is observed throughout the matrix, meaning that part of the Al is tied up in this phase. This would reduce the synergic effect for the mix with β clinker, but the opposite is observed.
   In total it is a balance between several effects and which is dominating.

3. Q: The strength increase observed when replacing 5% D fly ash with 5% limestone powder is low for all the clinkers (see Fig. 14)
   A: Fly ash D (STEAG) contains higher amounts of sulphates which leads to the formation of ettringite. This reduces the synergetic effect as ettringite (AFt) is stable versus calcium carbonate, while monosulphoaluminate (sulphate-AFm) is not.

4 CONCLUSIONS

4.1 Reasons for why clinker δ give higher strength than the other clinkers

Clinker δ gives higher early strength than the other clinkers because it contains anhydrite as flux and therefore has a total higher calcium sulphate content than the other cement when the same amount of gypsum is added to the clinkers o make cements.

Clinker δ also has a higher C_3A content (≈ 6%) than predicted from the Rietveld analysis and part of it probably as a glassy XRD amorphous phase with some fluorine.

Clinker δ only has a marginally higher surface than the other clinkers, but substantially higher C_3S content that will add to the higher early strength together with excess calcium sulphate not bound early by C_3A being able to help accelerate C_3S hydration.

The other clinkers contain a substantial amount of C_4AF that is very slowly reactive and substantial amounts has still not reacted at 28 days and thereby not contributed to strength.

4.2 Reasons for why fly ash D leads to higher strength than the other fly ashes

Fly ash D is not a real fly ash, but a fluidized bed ash that consist of a much more open structure than the closed glassy, spherical particles of the other fly ashes. It also contains a lot more calcium oxide (17.9% CaO) than the other fly ashes (Fly ash B is the second highest with 7.1% CaO). Hence it is assumed to be more reactive than the other ashes.

Fly ash D also contains considerable more sulphate (6.6% as SO_3) than the other fly ashes (fly ash B is the second highest with 0.5% SO_3) which would lead to more ettringite formed on the expense of AFm resulting in more water bound and hence higher strength.

The higher sulphate content (and partly less aluminate) for fly ash D compared to the other fly ashes also leads to a less response of this fly ash to the synergy effect with limestone.

References

[1] K. De Weerdt and H. Justnes; "Fly Ash-Limestone Synergy in Ternary Cements", COIN report, 2013.

SINTEF Building and Infrastructure is the third largest building research institute in Europe. Our objective is to promote environmentally friendly, cost-effective products and solutions within the built environment. SINTEF Building and Infrastructure is Norway's leading provider of research-based knowledge to the construction sector. Through our activity in research and development, we have established a unique platform for disseminating knowledge throughout a large part of the construction industry.

COIN – Concrete Innovation Center is a Center for Research based Innovation (CRI) initiated by the Research Council of Norway. The vision of COIN is creation of more attractive concrete buildings and constructions. The primary goal is to fulfill this vision by bringing the development a major leap forward by long-term research in close alliances with the industry regarding advanced materials, efficient construction techniques and new design concepts combined with more environmentally friendly material production.